

A NUMERICAL APPROACH TO BLOW-UP ISSUES FOR DISPERSIVE PERTURBATIONS OF BURGERS' EQUATION

CHRISTIAN KLEIN AND JEAN-CLAUDE SAUT

ABSTRACT. We provide a detailed numerical study of various issues pertaining to the dynamics of the Burgers equation perturbed by a weak dispersive term: blow-up in finite time versus global existence, nature of the blow-up, existence for “long” times, and the decomposition of the initial data into solitary waves plus radiation. We numerically construct solitons for fractionary Korteweg-de Vries equations.

1. INTRODUCTION

This paper is concerned with the numerical study of the dynamics and blow-up issues for “weak” dispersive perturbations of Burgers’ (inviscid) equation. As in [37] the motivation is to study the influence of dispersion on the dynamics of solutions to the Cauchy problem for “weak” dispersive perturbations of hyperbolic quasilinear equations or systems, as for instance the Boussinesq systems for surface water waves.

We thus want to investigate the competition between nonlinearity and dispersion. Usually this problem is attacked by fixing the dispersion, *eg* that of the Korteweg- de Vries (KdV) equation and varying the nonlinearity $u^p u_x$ in the generalized KdV (gKdV) equation

$$(1) \quad u_t + u^p u_x + u_{xxx} = 0.$$

However it is probably more physically relevant to fix the quadratic nonlinearity (*eg* uu_x) and to vary (lower) the dispersion. In fact in many problems arising from Physics or Continuum Mechanics, the nonlinearity is quadratic, with terms like $(u \cdot \nabla)u$ and the dispersion is in some sense weak. On the other hand, dispersive terms occuring in the Schrödinger or in the KdV equations are obtained by a Taylor expansion of the true dispersion at a given wave number k_0 or in the long wave limit. This allows strong dispersive effects (and nice mathematical properties!), but restricts the range of frequencies for which the model is relevant. For instance the dispersion relation of the KdV equation is a bad approximation of the one of the water waves for not too small frequencies. We refer to [34] for examples of water wave models with “full dispersion”, that is models which share the same dispersion as that of the water waves system. In particular the original dispersion is not strong enough for yielding the dispersive estimates that allows

to solve the Cauchy problem in relatively large functional classes (like the KdV or Benjamin-Ono equation in particular), down to the energy level for instance.¹

In fact many nonlinear dispersive systems have the following structure

$$(2) \quad \partial_t U + \mathcal{B}U + \epsilon \mathcal{A}(U, \nabla U) + \epsilon \mathcal{L}U = 0,$$

where the order 0 part $\partial_t U + \mathcal{B}U$ is linear hyperbolic, \mathcal{L} being a linear (not necessarily skew-adjoint) dispersive operator and $\epsilon > 0$ is a small parameter which measures the (comparable) nonlinear and dispersive effects. Both the linear part and the dispersive part may involve nonlocal terms (see *eg* [51], [46]).

Boussinesq systems for surface water waves (see [4, 5]) are important examples of somewhat similar systems. Note however that the Boussinesq systems (3) below cannot be reduced exactly to the form (2) except when $b = c = 0$. Otherwise the presence of a “BBM like” term induces a smoothing effect on one or both nonlinear terms. They read

$$(3) \quad \begin{cases} \partial_t \eta + \operatorname{div} \mathbf{v} + \epsilon \operatorname{div}(\eta \mathbf{v}) + \epsilon(a \operatorname{div} \Delta \mathbf{v} - b \Delta \eta_t) = 0 \\ \partial_t \mathbf{v} + \nabla \eta + \epsilon \frac{1}{2} \nabla(|\mathbf{v}|^2) + \epsilon(c \nabla \Delta \eta - d \Delta \mathbf{v}_t) = 0 \end{cases}, \quad (x_1, x_2) \in \mathbb{R}^2, t \in \mathbb{R}.$$

where a, b, c, d are modelling constants satisfying the constraint $a + b + c + d = \frac{1}{3}$ and ad hoc conditions implying the well-posedness of the linearized system at the trivial solution $(0, \mathbf{0})$.

When $b > 0, d > 0$, the dispersion in (3) is “weak” (the corresponding linear operator is of order $-1, 0$ or 1 (see [5]) contrary to the case $b = d = 0$, $a < 0, c < 0$ when it is of order 3 as in the KdV equation).

We will not address the blow-up issues for (3), which are completely open, but instead focus on one dimensional scalar equations.

More precisely, the major question addressed here will be whether or not smooth solutions of the Cauchy problem for weak dispersive perturbations of Burgers’ equation develop singularities in finite time and if blow-up occurs, what is its nature: a shock like in solutions to Burgers’ equation, a blow-up similar to the one of the L^2 critical or supercritical generalized KdV equations, or an “energy critical or super critical” blow-up, a case that never occurs for the generalized KdV equations (see below for a more detailed discussion).

We will also consider the *long time existence* issues, that is what is the qualitative behavior of the solution when it is global, or before the blow-up time if not; in particular does it show a decomposition into solitary waves plus radiation, a typical behavior of solutions to integrable equations such as the KdV equation? Also when global existence is not assured, how does the presence of a “weak” dispersive term affect the life span of the solution

¹And thus obtaining *global well-posedness* from the conservation laws.

to the underlying Burgers equation when a small parameter ϵ appears in front of the quadratic term and possibly in front of the dispersive terms?

The last question is particularly important for the complete rigorous justification of water waves models (see [34]). It is worth noticing that except when the solution is global (which can be proven essentially only for scalar one-way models) the only long time existence results for water waves models such as the Boussinesq systems (3) are established on the “hyperbolic” time scale $1/\epsilon$ (see [41, 51, 45, 46]). We will not address this issue in the context of relevant water waves models but again for the fractionary KdV or BBM (fKdV or fBBM) equations which will serve as toy models.

The paper is organized as follows: in section 2 we collect some analytically known facts about the equations to be studied numerically. The above questions will then be addressed for these equations numerically in section 3. We add some concluding remarks in section 4.

Notations. The following notations will be used throughout this article. The Fourier transform of a function f will be denoted \hat{f} or $\mathcal{F}f$. For any $s \in \mathbb{R}$, we define $D^s f$ by $\widehat{D^s f}(\xi) = |\xi|^s \hat{f}(\xi)$.

For $1 \leq p \leq \infty$, $L^p(\mathbb{R})$ is the usual Lebesgue space with the norm $\|\cdot\|_{L^p}$, and for $s \in \mathbb{R}$, the Sobolev space $H^s(\mathbb{R})$ is defined via its usual norm $\|f\|_{H^s} = (\int_{\mathbb{R}} (f^2 + |D^s f|^2) dx)^{1/2}$.

2. THEORETICAL PRELIMINARIES

In this section we gather known facts about various dispersive regularizations of Burgers' equation. In particular we consider fractionary KdV and BBM equations. We formulate analytic questions which will then be addressed numerically in the following section.

2.1. Fractionary KdV equations. We will thus focus as a paradigm on one-dimensional model equations. A first one (introduced by Whitham [50]) is of KdV type with a weak dispersion.

$$(4) \quad u_t + uu_x + \int_{-\infty}^{\infty} k(x-y)u_x(y,t)dy = 0.$$

This equation can also be written in the form

$$(5) \quad u_t + uu_x - Lu_x = 0,$$

where the Fourier multiplier operator L is defined by

$$\widehat{Lf}(\xi) = p(\xi)\hat{f}(\xi),$$

with $p = \hat{k}$.

In the original Whitham equation, the kernel k was given by

$$(6) \quad k(x) = \frac{1}{2\pi} \int_{\mathbb{R}} \left(\frac{\tanh \xi}{\xi} \right)^{1/2} e^{ix\xi} d\xi,$$

that is $p(\xi) = \left(\frac{\tanh \xi}{\xi}\right)^{1/2}$, which corresponds to the phase velocity of purely gravitational waves. The Whitham equation is also the one-dimensional version of the Full dispersion Kadomtsev-Petviashvili equation (FDKP) studied in [35]. When surface tension is added, the above p has to be changed to $p_S(\xi) = (1 + \beta|\xi|^2)^{1/2} \left(\frac{\tanh \xi}{\xi}\right)^{1/2}$, where $\beta \geq 0$ measures the surface tension effects. This leads to the extended Whitham equation.

We will consider here a family of equations where $p(\xi) = |\xi|^\alpha$, that we call “fractionary KdV equations”. The case $\alpha = 2$ corresponds to the usual KdV equation, $\alpha = 1$ to the Benjamin-Ono equation. It is well known (see [18]) that for $\alpha \geq 1$ the solutions of the Cauchy problem (in appropriate functional spaces) are global and therefore no finite time blow-up occurs. In the KdV case, it is known that the solution decomposes into solitons traveling to the right and radiation going to the left.

The case $\alpha < 1$ is more delicate, and we will focus on it.

When $-1 < \alpha < 0$, a blow-up occurs, that is there is a finite time blow-up of the solution of the Cauchy problem corresponding to suitable smooth initial data (see [9] and [10, 22, 42] for related equations). The proof in [9] extends easily to the Whitham equation (see [35]). By contradiction one proves that the $C^{1+\alpha}$ norm of a solution blows up in finite time, but the proof does not indicate whether the gradient only or both the solution and its gradient blow up.

The occurrence of a possible blow-up when $0 < \alpha < 1$ is an open problem. It is claimed in [32] without proof that then a shock formation is not possible.

We briefly recall here the known results for the associated Cauchy problem, that is

$$(7) \quad u_t + uu_x - D^\alpha u_x = 0, \quad u(., 0) = u_0,$$

where $\widehat{D^\alpha f}(\xi) = |\xi|^\alpha \hat{f}(\xi)$.

The following quantities are formally conserved by the flow associated to (7),

$$(8) \quad M(u) = \int_{\mathbb{R}} u^2(x, t) dx,$$

and the Hamiltonian

$$(9) \quad H(u) = \int_{\mathbb{R}} \left(\frac{1}{2} |D^{\frac{\alpha}{2}} u(x, t)|^2 - \frac{1}{6} u^3(x, t) \right) dx.$$

Note that by the Sobolev embedding $H^{\frac{1}{6}}(\mathbb{R}) \hookrightarrow L^3(\mathbb{R})$, $H(u)$ is well-defined when $\alpha \geq \frac{1}{3}$ but it does not make sense when $u \in H^{\alpha/2}(\mathbb{R})$, $\alpha < \frac{1}{3}$, the *energy super critical case*.

Moreover, equation (7) is invariant under the scaling transformation

$$(10) \quad u_\lambda(x, t) = \lambda^\alpha u(\lambda x, \lambda^{\alpha+1} t),$$

for any positive number λ . A straightforward computation shows that $\|u_\lambda\|_{\dot{H}^s} = \lambda^{s+\alpha-\frac{1}{2}}\|u\|_{\dot{H}^s}$, and thus the critical index corresponding to (7) is $s_\alpha = \frac{1}{2} - \alpha$. In particular, equation (7) is L^2 -critical for $\alpha = \frac{1}{2}$. This corresponds to $p = 4$ in the generalized KdV equation (1).

Compactness arguments (see [44]) prove that (7) admit global weak solutions (without uniqueness) in $L^\infty(\mathbb{R}; H^{\alpha/2}(\mathbb{R}))$ when $\alpha > \frac{1}{2}$ for initial data in $H^{\alpha/2}(\mathbb{R})$ (with a smallness condition when $\alpha = \frac{1}{2}$) and, thanks to a Kato type smoothing effect global weak solutions in $L^\infty(\mathbb{R}; L^2(\mathbb{R})) \cap L^2_{\text{loc}}(\mathbb{R}; H^{\alpha/2}_{\text{loc}}(\mathbb{R}))$, see [16, 17].

By using standard energy methods and the fact that the dispersive term is skew-adjoint (thus without using explicitly the dispersion), one can on the other hand prove that the Cauchy problem associated to (7) is locally well-posed in $H^s(\mathbb{R})$ for $s > \frac{3}{2}$, which is the same “hyperbolic type” result as for the Burgers equation.

Taking into account the dispersion, it has been established in [37] that the Cauchy problem for (7) is locally well posed for initial data in $H^s(\mathbb{R})$, for $s > s_\alpha = \frac{3}{2} - \frac{3\alpha}{2} > \frac{\alpha}{2}$, which does not allow to globalize the solution using the conservation laws.

It is well known that the solitary waves play a significant role in the dynamics of the KdV equation and one can ask whether or not this is the case for the dispersive Burgers equation.

A (localized) solitary wave solution of (7) of the form $u(x, t) = Q_c(x - ct)$ must satisfy the equation

$$(11) \quad D^\alpha Q_c + cQ_c - \frac{1}{2}Q_c^2 = 0,$$

where $c > 0$.

One does not expect solitary waves to exist when $\alpha < \frac{1}{3}$ since then the Hamiltonian does not make sense (see a formal argument in [32] and a rigorous proof in [37] which also proves nonexistence of solitary waves when $\alpha < 0$).

On the other hand solitary waves exist when $\alpha > \frac{1}{3}$ (see [11, 13, 14, 15]) and they have a slow decay for $|x| \rightarrow \infty$ as $\frac{1}{x^{1+\alpha}}$. They are expected to be orbitally stable when $\alpha > \frac{1}{2}$, that is in the L^2 subcritical case (this would correspond to $p < 4$ for the generalized KdV equations (1)). It is also worth noticing that solitary waves exist for the original Whitham equation ([11]). The proof uses in a crucial way that the dispersion relation of the Whitham equation approaches that of the KdV equation for small frequencies.

Note that the exponent $\alpha = \frac{1}{3}$ corresponds to the so-called “energy critical case” that never occurs for the generalized KdV equations where the energy (Hamiltonian) always makes sense in the energy space $H^1(\mathbb{R})$.

At this stage, one could make the following conjectures for (7) when $0 < \alpha < 1$:

1. No hyperbolic blow-up exists (no blow-up of the spatial gradient with bounded sup-norm).

2. When $\frac{1}{2} < \alpha < 1$, the solution is global (no blow-up).

3. When $\frac{1}{3} < \alpha \leq \frac{1}{2}$, which is the L^2 supercritical case, one has a “nonlinear dispersive blow-up”, with a kind of self-similar structure. This would correspond to $p \geq 4$ for the generalized KdV equation. Recall that this type of blow-up for (1) is supported by numerical simulations in the super critical case $p > 4$ ([6, 29], and in the critical case $p = 4$ [29] and rigorously proven in the critical case $p = 4$ ([39]). The dynamics of the blow-up is different in the L_2 -critical and in L_2 -supercritical cases.

4. When $0 < \alpha < \frac{1}{3}$, the energy critical case which has no counterpart for the generalized KdV equations, one expects a blow-up, but with a different structure of that of the previous case.

2.2. Fractionary BBM equations. We now turn to the BBM version of the dispersive Burgers equation, namely

$$(12) \quad \partial_t u + \partial_x u + u \partial_x u + D^\alpha \partial_t u = 0,$$

where the operator D^α is defined as previously.

The case $\alpha = 2$ corresponds to the classical BBM equation, $\alpha = 1$ to the BBM version of the Benjamin-Ono equation.

For any α the energy

$$(13) \quad E(t) = \int_{\mathbb{R}} (u^2 + |D^{\frac{\alpha}{2}} u|^2) dx$$

is formally conserved. By a standard compactness method, this implies that the Cauchy problem for (12) admits a global weak solution in $L^\infty(\mathbb{R}; H^{\frac{\alpha}{2}}(\mathbb{R}))$ for any initial data $u_0 = u(\cdot, 0)$ in $H^{\frac{\alpha}{2}}(\mathbb{R})$.

One can also use the equivalent form

$$(14) \quad \partial_t u + \partial_x (I + D^\alpha)^{-1} \left(u + \frac{u^2}{2} \right) = 0,$$

which gives the Hamiltonian formulation

$$u_t + J_\alpha \nabla_u H(u) = 0$$

where the skew-adjoint operator J_α is given by $J_\alpha = \partial_x (I + D^\alpha)^{-1}$ and $H(u) = \frac{1}{2} \int_{\mathbb{R}} (u^2 + \frac{1}{3} u^3)$. Note that the Hamiltonian makes sense and is formally conserved for $u \in H^{\frac{\alpha}{3}}(\mathbb{R})$ if and only if $\alpha \geq \frac{1}{3}$.

We will again focus on the case $0 < \alpha < 1$. Actually when $\alpha \geq 1$, (14) is an ODE in the Sobolev space $H^s(\mathbb{R})$, $s > \frac{1}{2}$, and one obtains by standard arguments (see [38, 3]) the local well-posedness of the Cauchy problem in

$H^s(\mathbb{R})$, $s > \frac{1}{2}$. When $\alpha = 1$ (the Benjamin-Ono BBM equation), the conservation of energy and an ODE argument as in [44] or the Brézis-Gallouët inequality implies that this local solution is in fact global.

The following local well-posedness result is established in [37].

Theorem 1. *Let $0 < \alpha < 1$. Then the Cauchy problem for (12) or (14) is locally well-posed for initial data in $H^r(\mathbb{R})$, $r > r_\alpha = \frac{3}{2} - \alpha$.*

It is clear from the formulation (14) that the fractionary BBM equation is for $0 < \alpha < 1$ a different dispersive perturbation of the Burgers equation of that given by the fractionary KdV equation: roughly speaking, one replaces the ∂_x derivative of $u + \frac{u^2}{2}$ by a derivative of order $1 - \alpha$.

The question is now: Is there a blow-up when $0 < \alpha < 1$ and if yes, what is its nature?

2.3. Large time existence issues. An important issue, when the solution is global, is to describe its qualitative behavior. In the range of fKdV equations, the only fully understood case is $\alpha = 2$, the KdV equation where Inverse Scattering techniques yield a full description of the solution. For the other values of α , such a description is not known (the only other integrable equation in the family corresponds to $\alpha = 1$, the Benjamin-Ono equation, but then Inverse Scattering techniques only work for small initial data). One aim of our numerical simulations is to investigate what happens when $\frac{1}{2} < \alpha < 1$. They actually suggest that a kind of *decomposition into solitary waves plus radiation* occurs, despite the fact that none of those equations are integrable. A similar behavior seems to hold for the fBBM equations, at least when $\alpha > \frac{1}{3}$.

Another interesting and widely open question is to investigate the influence of a weak dispersion on the existence time of solutions to hyperbolic equations or systems (see [45, 46, 51] for some partial answers in the case of various water wave systems, in particular the Boussinesq systems).

Again a simple relevant example is the dispersive Burgers equation

$$(15) \quad u_t + \epsilon u u_x - \epsilon D^\alpha u_x = 0, \quad u(., 0) = u_0,$$

where ϵ is a small positive parameter (in the water waves context it could model the comparable effects of dispersion and nonlinearity).

Since the dispersive term in (15) is skew-adjoint, one immediately deduces that for initial data u_0 of order 1 in say $H^s(\mathbb{R})$, $s > \frac{3}{2}$, the solution exists on time scales of order $\frac{1}{\epsilon}$.

By changing the time variable as $\tau = \epsilon t$ one eliminates the ϵ 's from (15), that is one obtains

$$(16) \quad u_\tau + u u_x - D^\alpha u_x = 0, \quad u(., 0) = u_0,$$

and we have the following dichotomy:

- Either the solution to (16) is global and so is that of (15),

• or the solution to (16) has a lifespan of order $O(1)$ and that of (15) has a lifespan of order $O(1/\epsilon)$, that is the same as for the Burgers equation.

Our simulations below suggest that when $\alpha > 1/2$ the first situation occurs while when $\alpha \leq 1/2$ the second one holds.

Things are more delicate when the small parameter appears only in front of the nonlinear term as shows the striking example of the Burgers-Hilbert equation

$$(17) \quad u_t + \epsilon u u_x + \mathcal{H}u = 0, \quad u(\cdot, t) = u_0$$

where \mathcal{H} is the Hilbert transform. It is established in [20, 21] that for initial data of order $O(1)$ the solution of (17) exists on time scales of order $\frac{1}{\epsilon^2}$ while the corresponding Burgers solution exists on time scales of order $\frac{1}{\epsilon}$.

One should thus consider the Cauchy problem

$$(18) \quad u_t + \epsilon u u_x - D^\alpha u_x = 0, \quad u(\cdot, 0) = u_0,$$

An equivalent formulation (by setting $v = \epsilon u$) is to consider the Cauchy problem

$$(19) \quad v_t + v v_x - D^\alpha v_x = 0, \quad v(\cdot, 0) = \epsilon u_0,$$

and the question is to see how the existence time $O(\frac{1}{\epsilon})$ is enlarged by the dispersive term $D^\alpha v_x$, in particular, is it possible to prove the existence of global small solutions to (19)? This would give an example of initial data leading to a shock for the Burgers equation and to a global solution for fKdV.

Of course similar questions can be addressed for the BBM version, that is

$$(20) \quad u_t + u_x + \epsilon u u_x + \epsilon D^\alpha u_t = 0, \quad u(\cdot, 0) = u_0,$$

or

$$(21) \quad u_t + u_x + \epsilon u u_x + D^\alpha u_t = 0, \quad u(\cdot, 0) = u_0,$$

Note that in (20) one cannot eliminate anymore the ϵ' 's by a change of time scale because of the transport term.

Similar issues for the Boussinesq systems (3) are widely open. Here (and for other relevant water waves models) no existence results beyond the “hyperbolic” time $\frac{1}{\epsilon}$ seem to be known (see [41, 51, 45, 46]). Recall that for the Boussinesq systems, the error estimates with the full water waves system being $O(\epsilon^2 t)$, (see [4]), and the solutions are expected to exist at least up to time scales of order $\frac{1}{\epsilon^2}$. There are here difficulties that are not present in the toy model fKdV or fBBM. First the change of time scale $\tau = \epsilon t$ does

not eliminate anymore the ϵ' 's in the system because of the order zero hyperbolic part. Moreover, as previously noticed, when b and/or d are strictly positive, the nonlinear term in the corresponding equation is smoothed by the operator $(I - b\Delta)^{-1}$, (resp. $(I - d\Delta)^{-1}$).

The case studied in [2, 47] (that is $a = b = c = 0, d = \frac{1}{3}$) is specially interesting since it was considered in those references as a perturbation of the (hyperbolic) Saint-Venant system.

3. NUMERICAL STUDY OF WEAKLY DISPERSIVE REGULARIZATIONS OF BURGERS' EQUATION

In this section we will study numerically solutions to fKdV, fBBM and Whitham equations. The focus will be on smooth, localized initial data for which we study the decomposition into solitons and a possible blow-up in finite time. We also address the long time behavior of small initial data. First we will present the used numerical tools and discuss how accuracy is ensured. Then we will study concrete examples.

3.1. Numerical Methods for the time evolution. Since the equations to be studied in this paper contain fractionary derivatives being defined as Fourier multipliers, it is convenient to use Fourier spectral methods in the numerical treatment. We concentrate on rapidly decreasing, smooth initial data which can be analytically continued within the finite numerical precision as periodic functions. In other words, we use large enough computational domains that the Fourier coefficients of the periodically continued initial data decrease to machine precision (10^{-16} in our case). The fractional derivatives for Fourier series are defined in analogy to the definition for Fourier transforms. The discrete Fourier transform is computed via a *fast Fourier transform* (fft).

The fKdV equation for the Fourier transform \hat{u} of u has the form

$$(22) \quad \hat{u}_t = \mathcal{F}(u) + \mathcal{L}\hat{u},$$

where $\mathcal{L} = i\xi|\xi|^\alpha$ is a linear operator², and where $\mathcal{F}(u) = -i\widehat{\xi u^2}/2$ denotes the nonlinear terms. It is an advantage of Fourier methods that the x -derivatives and thus the operator \mathcal{L} are diagonal. For equations of the form (22) with diagonal \mathcal{L} , there are many efficient high-order time integrators, see e.g. [25, 19, 28, 30] and references therein. This allows for an efficient integration in time.

In [29] it was shown that an implicit Runge-Kutta method of fourth order (IRK4), a two-stage Gauss scheme, is both very efficient and accurate up to blow-up for generalized KdV equations. For the initial value problem $y' = f(y, t)$, $y(t_0) = y_0$ and constant time steps t_m , $m = 0, 1, \dots$ with

²For the Whitham equation (4), the symbol $|\xi|^\alpha$ is simply replaced with $\sqrt{\tanh(\xi)}/\xi$.

$t_{m+1} - t_m = h$ and $y(t_m) = y_m$, this scheme has the form

$$(23) \quad y_{m+1} = y_m + \frac{h}{2}(K_1 + K_2),$$

$$(24) \quad K_i = f \left(t_m + c_i h, y_m + h \sum_{j=1}^s a_{ij} K_j \right), \quad i = 1, 2,$$

where $c_1 = \frac{1}{2} - \frac{\sqrt{3}}{6}$, $c_2 = \frac{1}{2} + \frac{\sqrt{3}}{6}$ and $a_{11} = a_{22} = 1/4$, $a_{12} = \frac{1}{4} - \frac{\sqrt{3}}{6}$, $a_{21} = \frac{1}{4} + \frac{\sqrt{3}}{6}$. The implicit equations for K_1 and K_2 are solved iteratively with a simplified Newton scheme,

$$(25) \quad \begin{pmatrix} K_1 \\ K_2 \end{pmatrix} = \begin{pmatrix} 1 - ha_{11}\mathcal{L} & -ha_{12}\mathcal{L} \\ -ha_{21}\mathcal{L} & 1 - ha_{22}\mathcal{L} \end{pmatrix}^{-1} \begin{pmatrix} \mathcal{F}(\hat{u}_m + h(a_{11}K_1 + a_{12}K_2)) + \mathcal{L}\hat{u}_m \\ \mathcal{F}(\hat{u}_m + h(a_{21}K_1 + a_{22}K_2)) + \mathcal{L}\hat{u}_m \end{pmatrix}.$$

Since the operator \mathcal{L} is diagonal, the inverse matrix on the right-hand side of (25) can be given explicitly. In this form the iteration converges rapidly (at early times in 3 to 4 iterations).

The fBBM equation (12) reads in Fourier space

$$\hat{u}_t = -\frac{i\xi}{1 + |\xi|^\alpha}(\hat{u} + \widehat{u^2}/2),$$

which is again integrated with the IRK4 method.

Accuracy of the numerical solution is controlled as discussed in [28, 30, 29] via the numerically computed energies (9) and (13) which will depend on time due to unavoidable numerical errors. We use the quantity

$$(26) \quad \Delta = |E(t)/E(0) - 1|$$

as an indicator of the numerical accuracy. It was shown in [28, 30] that the numerical accuracy of this quantity overestimates the L_∞ norm of the difference between numerical and exact solution by two to three orders of magnitude. A precondition for the usability of this quantity is a sufficient resolution in Fourier space.

Dynamic rescaling. To study blow-up in the solutions to fKdV, the scale invariance (10) can be used as for gKdV and NLS equations in the form of a dynamic rescaling, see for instance [49, 29] and references therein. To this end the constant λ in (10) is replaced with a t -dependent function $L(t)$

$$(27) \quad y = \frac{x - x_m}{L}, \quad \frac{d\tau}{dt} = \frac{1}{L^{1+\alpha}}, \quad U = L^\alpha u.$$

As in [29] for gKdV, we take into account the fact that the peak at $x = x_m(t)$ developing eventually into a blow-up is travelling with increasing speed. To address this, we choose a commoving frame. Equation (27) implies for (7)

$$(28) \quad U_\tau - (\ln L)_\tau (\alpha U + y U_y) - \frac{x_{m,\tau}}{L} U_y + U U_y - D_y^\alpha U_y = 0.$$

The scaling function L can be chosen to keep certain norms constant, for instance the L_∞ -norm. It appears that the choice to keep the L_2 norm of

U_y constant is numerically preferred for stability reasons. This choice leads to

$$(29) \quad a := (\ln L)_\tau = \frac{1}{(2\alpha + 1)\|U_y\|_2^2} \int_{\mathbb{R}} U^2 U_{yyy} dy.$$

Since $y = 0$ is supposed to be an extremum of the solution, we have $U_y(0, \tau) = 0$ and $U_{yy}(0, \tau) = 0$. Putting $U(0, 0, \tau) = U_0 = \text{const}$, we get from (28) for the speed $v = x_{m, \tau}/L$

$$(30) \quad v = U_0 + \frac{1}{U_{yy}(0, \tau)} (D^\alpha U_y)(0, \tau).$$

Thus all quantities in (28) can be expressed in terms of U alone. In the case of an L_∞ blow-up for $t = t^*$, the scaling function L is expected to vanish for $\tau \rightarrow \infty$. Thus for $t \rightarrow t^*$, both x and t are dynamically rescaled. Note that for solutions of this equation the energy

$$(31) \quad E[U] = \frac{1}{L^{1-3\alpha}} \int_{\mathbb{R}} (U^2 + |D^{\frac{\alpha}{2}} U|^2) dy$$

is conserved. It can be seen that the case $\alpha = 1/3$ is energy critical in the sense that it is invariant under the rescaling (28).

For $\tau \rightarrow \infty$, it is expected that the solution U to the rescaled equation (28) as well as $a \rightarrow a_\infty$ and $v \rightarrow v_\infty$ become τ independent (this behavior was proven in [40] for the L_2 critical gKdV equation for initial data in the vicinity of a soliton). In this case equation (28) reduces to an ordinary fractionary differential equation

$$(32) \quad -a_\infty (\alpha U^\infty + y U_y^\infty) - v_\infty U_y^\infty + U^\infty U_y^\infty - D_y^\alpha U_y^\infty = 0.$$

If a_∞ vanishes, this is exactly the equation (11) for the soliton. A blow-up of this type would be asymptotically given by a rescaled solution of equation (32).

In [29] it was shown numerically that generic rapidly decreasing hump-like initial data for gKdV lead to a tail of dispersive oscillations towards infinity with slowly decreasing amplitude. Due to the imposed periodicity, these oscillations reappear after some time on the opposing side of the computational domain and lead to numerical instabilities in the dynamically rescaled equation. The source of these problems is the term $y U_y$ in (28) since y is large at the boundaries of the computational domain. This implies that this term is very sensitive to numerical errors. For gKdV this could be addressed by using high resolution in time and large computational domains. It turns out that for fKdV, the dispersive oscillations have an amplitude that decreases even more slowly towards infinity. Thus we could not compute long enough to get conclusive results. Instead we integrate fKdV as described above directly, and then we use some postprocessing to characterize the type of blow-up via the above rescaling. We read off the time evolution of the

quantity L as defined via the L_2 norm of the gradient,

$$(33) \quad \frac{\|U_y\|_2}{\|u_x\|_2} = L^{\alpha+1/2},$$

where the constant $\|U_y\|_2$ is chosen to be $\|u_x(x, 0)\|_2$. This allows to study the type of the blow-up for fKdV in a similar way as for gKdV in [29] without actually solving equation (28). We ensure that the numerically computed energy of the solution is conserved to a certain precision ($\Delta < 10^{-3}$ in (26)), that there is sufficient resolution in Fourier space and in time for all computed times close to the blow-up time t^* . We generally choose the time step in blow-up scenarios such that the accuracy is limited by the resolution in Fourier space, i.e., that a further reduction of the time step for a given number of Fourier modes does not change the final result within numerical accuracy.

For gKdV, essentially two cases were relevant for the τ -dependence of the scaling factor L , and we want to test whether the same is true for fKdV. In the L_2 -critical case, one has $L \propto \tau^{-\gamma}$ with $\gamma = 1$. An algebraic decrease of L close to blow-up implies with (27) for fKdV

$$(34) \quad \|u_x\|_2^2 \propto (t^* - t)^{-\frac{2\alpha+1}{1+\alpha-1/\gamma}}, \quad \|u\|_\infty \propto (t^* - t)^{-\frac{\alpha}{1+\alpha-1/\gamma}}.$$

In the supercritical case for gKdV ($n > 4$), there does not exist a proof yet, but it is expected that L vanishes exponentially with τ for $\tau \rightarrow \infty$, $L \propto \exp(-\kappa\tau)$ with κ a positive constant. This implies with (27)

$$(35) \quad \|u_x\|_2^2 \propto (t^* - t)^{-\frac{2\alpha+1}{1+\alpha}}, \quad \|u\|_\infty \propto (t^* - t)^{-\frac{\alpha}{1+\alpha}}.$$

It will be tested whether such scalings can be observed in the numerical experiments for fKdV.

Singularity tracing in the complex plane. An important question in the context of the numerical solution of nonlinear dispersive PDEs is the identification and the characterization of a blow-up of the solution. The task is to identify the appearance of a singularity of the solution. Since we use a Fourier approach here, a possible tool in this context is a method from asymptotic Fourier analysis first applied to numerically identify singularities in solutions to PDEs in [48]. The idea is to use the fact that a singularity of a real function in the complex plane of the form $U \sim (z - z_0)^\mu$ (μ not an integer) leads for $|\xi|$ large to a Fourier transform of the form (if this is the only singularity of this type in the complex plane)

$$(36) \quad |\hat{U}| \sim \frac{1}{\xi^{\mu+1}} e^{-\xi\delta}, \quad \xi \gg 1,$$

where $\delta = \Im z_0$. In [31] it was discussed how this approach can be used to quantitatively identify the time where the singularity hits the real axis, i.e., where the real solution becomes singular. In addition this method gives the quantity μ which characterizes the type of the singularity. It was shown in [31] that the quantity δ can be identified reliably from a fitting of the Fourier coefficients, whereas there is a larger inaccuracy in the quantity μ .

Thus the numerically determined values for μ have to be taken with a grain of salt.

Tests. Contrary to the case of the KdV equation, it is not known if for the BO and the BBM equation the solutions of the initial value problems for these equations decompose for large times into solitons and radiation. The reason is that the Inverse Scattering Transform technique for the BO equation works only for small initial data and that the BBM equation is not completely integrable. Nevertheless a similar behavior can be expected for fKdV and fBBM solution, and it is tempting to examine this issue. Solitons are very important in this context, and an accurate reproduction of these solutions for the cases where they are explicitly known is crucial. Equation (11) has for $\alpha = 1$ the solution

$$(37) \quad Q_c = \frac{4c}{1 + (cx)^2}.$$

This solution decreases as x^{-2} for $|x| \rightarrow \infty$ which is numerically problematic for the Fourier methods we use here. The algebraic decrease implies that the solution cannot be analytically continued within the given finite precision even on large domains. Thus a Gibbs phenomenon will appear which has the consequence that the Fourier coefficients do not decrease to machine precision. In other words the numerical precision will be limited because of this algebraic decrease. This is in contrast to gKdV equations, for which the solitons are explicitly known, and where they decrease exponentially for $|x| \rightarrow \infty$. We recall that for $\alpha < 1$ the soliton solutions of (11) decrease as $|x|^{-(1+\alpha)}$ for $|x| \rightarrow \infty$, see [15].

To numerically test the propagation of the soliton, we use Q_c in (37) as initial data for fKdV with $\alpha = 1$ and $c = 2$. The test is performed with $N = 2^{14}$ Fourier modes for $x \in 100[-\pi, \pi]$. The modulus of the Fourier coefficients decreases in this case to 10^{-8} . We propagate the initial data with $N_t = 10^4$ time steps to time $t = 1$. The numerically computed energy is conserved to the order of 10^{-14} , i.e., machine precision. But since the Fourier coefficients just decrease to the order of 10^{-8} , the accuracy of the solution cannot be higher than this value. In fact we find that the L_∞ norm of the difference between exact and numerical solution is of the order of 10^{-7} as indicated by the resolution in Fourier space. This shows that the code reproduces the exact solution with the precision available in Fourier space, and that it is crucial to provide enough resolution there to distinguish the formation of solitons from the appearance of a blow-up.

Travelling wave solutions of the fBBM equation satisfy again equation (11) after a change $c \rightarrow \tilde{c} = 1 - 1/c$ and $u \rightarrow u/c$. Thus for $\alpha = 1$, the fBBM equations have soliton solutions of the form

$$(38) \quad u(x, t) = \frac{4(c-1)}{1 + \tilde{c}^2(x - ct)^2}, \quad \tilde{c} = 1 - \frac{1}{c}.$$

If we choose the same c and the same parameters for the numerical solution as above, the modulus of the Fourier coefficients decreases only to 10^{-6} in this case since the initial data decrease even more slowly for $|x| \rightarrow \infty$ because of $\tilde{c} = 1/2$. The numerically computed energy is again conserved to the order of machine precision. But since the resolution in Fourier space is only of the order of 10^{-6} , the difference between the exact and the numerical solution for $t = 1$ is of the order of 10^{-5} as expected.

3.2. Numerical construction of solitons. In this subsection we numerically solve equation (11) to obtain solitons of the studied equations. Note that we can concentrate on the case $c = 1$ since the solution for general c follows from the former via the simple rescaling

$$(39) \quad Q_c(z) = cQ_1(zc^{1/\alpha}).$$

To simplify the notation we suppress the index of Q for $c = 1$.

We solve equation (11) for $c = 1$ as in the previous subsection in Fourier space, where it has the form

$$(40) \quad (|\xi|^\alpha + 1)\hat{Q} - \frac{1}{2}\widehat{Q^2} = 0.$$

In the numerical solution the Fourier transform is approximated as before via a discrete Fourier series computed via an fft. The task is thus to find the (nontrivial) zero of the function $F = (|\xi|^\alpha + 1)\hat{Q} - \frac{1}{2}\widehat{Q^2}$ depending on the vector \hat{Q} of the discrete Fourier transform of Q , which can in general only be done iteratively. A potential problem in this context is that equation (40) has the trivial solution $\hat{Q} = 0$, and a straight-forward fixed point iteration typically converges to this solution, even if one starts with an exact solution. Thus we use a Newton method in the standard form $\hat{Q}_{n+1} = \hat{Q}_n - \text{Jac}^{-1}F(\hat{Q}_n)$, where Jac is the Jacobian of (40).

A technical problem in this context is the slow decrease of the soliton solution for $|x| \rightarrow \infty$ which is known to be of the order $O(|x|^{-(1+\alpha)})$, see [15]. Since the function Q is treated as essentially periodic, it will not be smooth at the boundaries of the computational domain. This loss of smoothness implies an algebraic decrease of the modulus of the Fourier coefficients and thus a slower convergence rate of the numerical scheme. To address this we choose a large domain, $x \in 100[-\pi, \pi]$ and high resolution in Fourier space, $N > 2^{14}$. Since the Jacobian entering the Newton iteration is a $N \times N$ matrix, its inverse cannot be computed with conventional methods on a standard computer. Therefore we use Krylov-subspace techniques, here GMRES [43]. The idea is to compute the inverse of a matrix iteratively. The advantage of GMRES is that the to be inverted matrix does not have to be known explicitly, just its action on a vector. Thus to compute $\text{Jac}^{-1}F(\hat{Q}_n)$, we need only

$$\text{Jac}\hat{X} = (|\xi|^\alpha + 1)\hat{X} - \widehat{QX},$$

where X is some vector. The Newton iteration is stopped when the L_∞ norm of F is smaller than 10^{-8} . Generally we reach machine precision after 4-8 iterations if the initial iterate is chosen as explained below.

To test this approach we consider the BO soliton (37), i.e., the case $\alpha = 1$. We choose $N = 2^{14}$ and $1.1Q$ as the initial iterate, i.e., the exact solution multiplied with a factor 1.1. After 3 iterations we reach a residual $\|F\|_\infty$ of the order of 10^{-12} . It can be seen in Fig. 1 that the Fourier coefficients of the solution decrease to machine precision. In the same figure we also show the difference between numerical and exact solution which is of the order of 10^{-4} , the largest difference being observed at the maximum of the solution. The reason for this difference despite resolution in Fourier space and the solution of equation (40) to machine precision is the periodic setting we are using here. This also implies the increase of the difference towards the boundary of the domain. But the example indicates that we should be able to obtain the solitons of (11) to the order of plotting accuracy also for $\alpha < 1$.

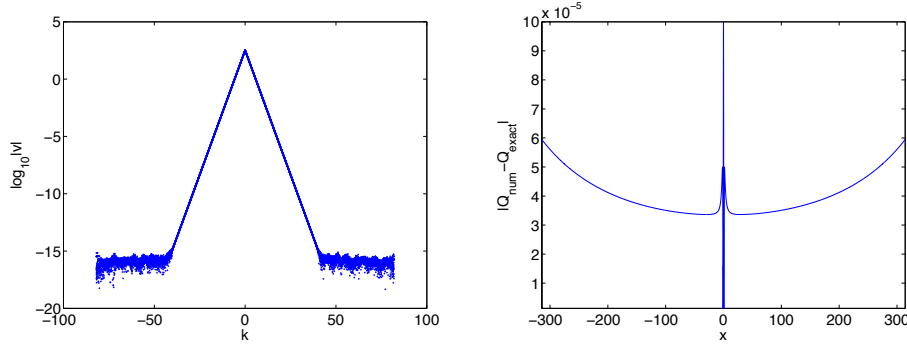


FIGURE 1. Modulus of the Fourier coefficients for the soliton (11) of the BO equation ($\alpha = 1$) with $c = 1$ on the left, and the difference of the numerical and the exact solution on the right.

To construct solitons for $\alpha < 1$, we use the solution for a given value of α as the initial iterate for equation (40) for a smaller value α : to construct the solution for $\alpha = 0.9$ for instance, we start with the BO soliton. By lowering α by 0.1 in this way, we can reach values of 0.6 without problems. For even smaller values of α , we have to take smaller steps in α , of the order of 0.01. The resulting solutions are shown in Fig. 2 for values of x close to the maximum.

It can be seen that the solutions become more and more peaked the smaller α is, and the decrease towards infinity becomes slower; the latter can be seen more clearly in Fig. 3, where the BO soliton intersects for larger x the solitons for smaller α . This is challenging for the numerical method, and we use $N = 2^{18}$ Fourier modes to provide the necessary resolution. In Fig. 3, it can be also seen that the modulus of the Fourier coefficients still

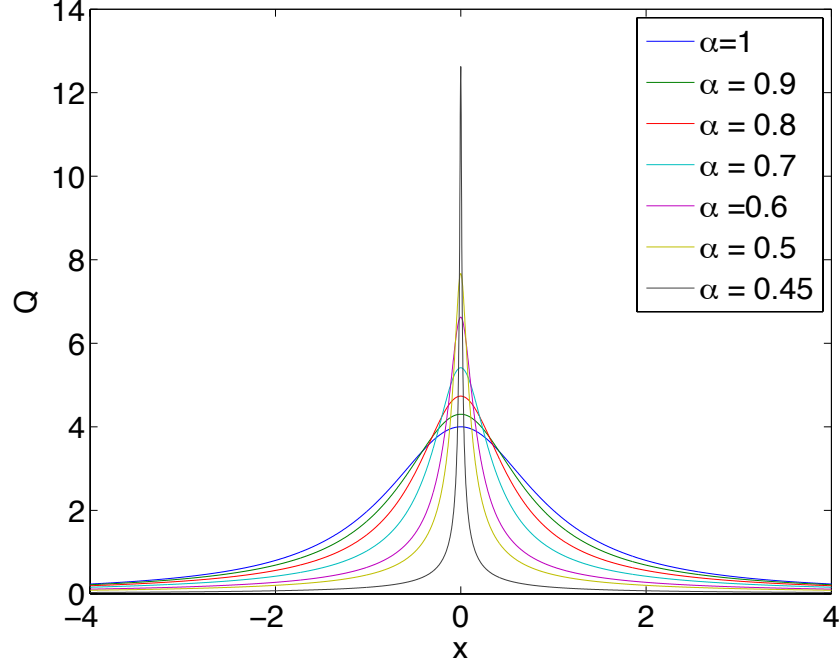


FIGURE 2. Solitary waves (11) for $c = 1$ and different values of α .

goes down to 10^{-4} in this case. To be able to increase the resolution further, it would be necessary at one point to use higher precision, i.e., quadruple instead of the used double precision. But given the strong increase of the maximum of the solution for decreasing α , it seems doubtful that one can reach much smaller values of α with this approach. The limit $\alpha = 1/3$ appears to be inaccessible in this way.

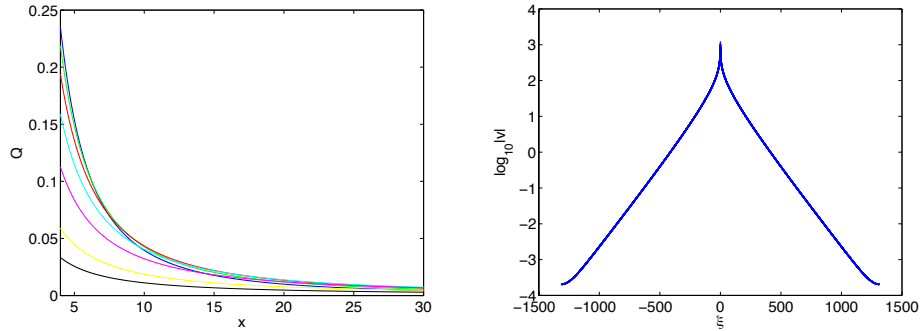


FIGURE 3. Solitons of Fig. 2 for larger values of x on the left, and the modulus of the Fourier coefficients for the soliton (11) with $c = 1$ and $\alpha = 0.45$ on the right.

In Fig. 4 we trace the mass and the energy of the solitons for $c = 1$ in dependence of α . It can be seen that the mass is monotonically increasing with α , whereas the energy decreases. For $\alpha = 0.5$ we get $M \sim 3.043$ and $E = -0.002$. The latter value is compatible with zero for the precision with which we determine the soliton.

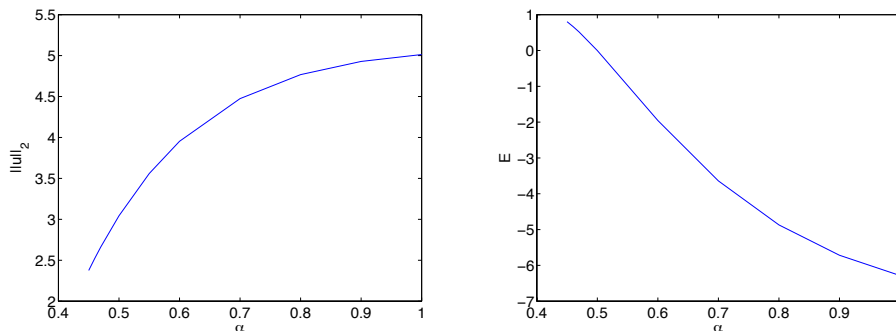


FIGURE 4. Mass (left) and energy (right) of the solitons in Fig. 2 in dependence of α .

It is possible to construct in a similar way solitons to the Whitham equation (4). These solitons satisfy equation (11) if one replaces D^α with the operator L in (5) having the Fourier symbol $\left(\frac{\tanh(\xi)}{\xi}\right)^{1/2}$. For small ξ , the Whitham equation reduces to the KdV equation in the form $u_t + uu_x - \frac{1}{6}u_{xxx} = 0$ which has the solitonic solution

$$(41) \quad Q_c = 3(c+1)\text{sech}^2(\sqrt{-1.5(c+1)}x).$$

Thus for real solutions one needs $c+1 < 0$ which implies that the soliton is negative and travelling to the left in contrast to the fKdV solitons considered above. For $c \rightarrow -1$ the amplitude of the soliton tends to zero. If we use the KdV soliton (41) for negative $c+1$ close to zero, the iteration for the Whitham soliton converges quickly. In Fig. 5 we show the Whitham and the KdV soliton for $c+1 = -1.2$. For smaller c the iteration stops converging. A numerical treatment of the solitary waves of the Whitham equation along similar lines has been already presented in [12]. There periodic solutions were treated which tend to solitons in the limit of large periods. In our case, the period is chosen large enough that the found solution (which is as the KdV soliton rapidly decreasing in contrast to the fKdV solitons) should be equal to the soliton within numerical accuracy. In [12] it was also shown that there is a maximal $|c|$ of the soliton due to the fact that the dispersion of the Whitham equation decreases with $|c|$. Note that the Whitham equation in [12] is not written in dimensionless coordinates as here, and that the dispersion has a different sign. It is clear that the maximal $|c|$ we observe for the iteration to converge is related to the nonexistence of solitons of the Whitham equation for large speeds. But we cannot say how close we get

to the limiting velocity since failure of an iteration to converge can also be related to an inadequate initial iterate.

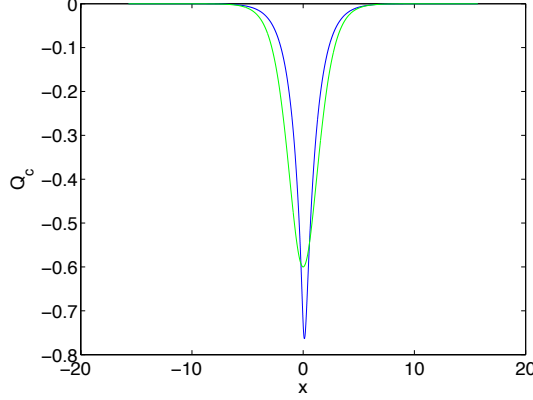


FIGURE 5. Soliton of the Whitham equation for $c = -1.2$ in blue and the corresponding KdV soliton in green.

3.3. Numerical study of blow-up in fractionary KdV equations.

In this subsection we will study numerically the possibility of blow-up in fKdV equations. We concentrate on the case $0 < \alpha < 1$ and the initial data $u_0 = \beta \text{sech}^2 x$ which are motivated by the KdV soliton. Since these initial data are rapidly decreasing, they can be treated as essentially periodic as discussed above. We find that solutions for sufficiently large β decompose for $\alpha > 1/2$ asymptotically into solitons and radiation. For $\alpha = 1/2$, we find blow-up for initial data with negative energy. The blow-up profile is given by a dynamically rescaled soliton as for the L_2 critical case for gKdV. In the supercritical case with $1/3 < \alpha < 1/2$, we find blow-up for initial data with sufficiently large mass similar to the supercritical blow-up in gKdV. In the energy supercritical case $\alpha \leq 1/3$, there will be again blow-up, but since there are no solitons in this case, there will be no formation of a soliton which finally blows up, but the initial hump steepens as known from the Burgers' equation and finally blows up.

We first study an example for $\alpha = 0.6$, i.e., $1/2 < \alpha < 1$. No blow-up is expected in this case. For the initial data $u_0 = 5 \text{sech}^2 x$, we get the solution shown in Fig. 6. The initial hump gets laterally compressed and increases in height. At a given point it splits into two humps which both continue to grow in height. The humps seem to approach solitons since their speed becomes almost constant after some time and their shape stops changing. Thus it appears that an initial pulse of sufficient size decomposes into solitons. The remaining energy is radiated away in the form of oscillations propagating to the left whilst the humps travel to the right. The computation is carried out with $N = 2^{14}$ Fourier modes for $x \in 7[-\pi, \pi]$ and $N_t = 10^4$ time steps. The relative energy is conserved to the order of 10^{-12} .

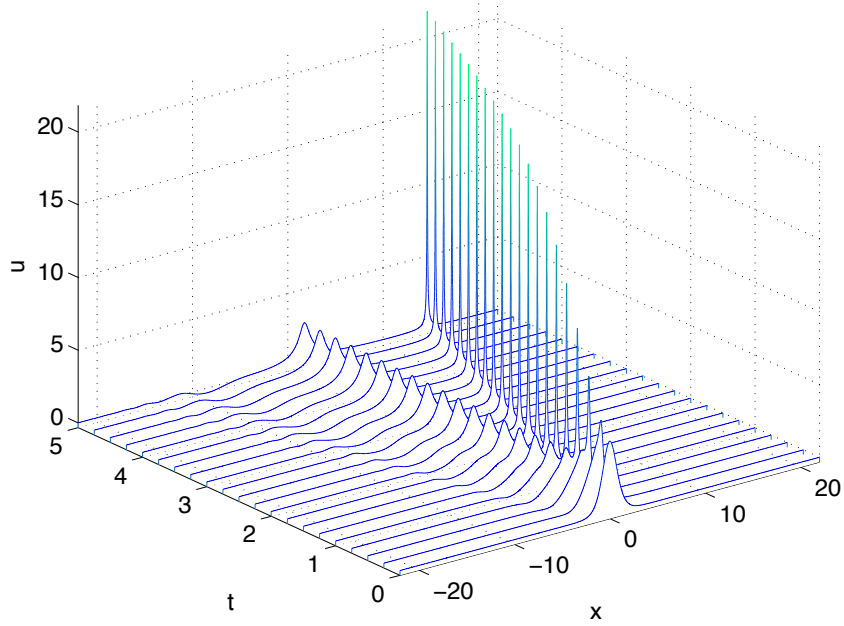


FIGURE 6. Solution to the fKdV equation (7) for $\alpha = 0.6$ and the initial data $u_0 = 5\text{sech}^2 x$.

Note that the dispersive oscillations in Fig. 6 decay only very slowly in amplitude. Due to the imposed periodic boundary conditions, this leads to oscillations also to the right of the initial hump where there would be none on an infinite domain. A consequence of these oscillations are small oscillations in the L_∞ norm of the solution in Fig. 6 which is shown in Fig. 7. Nonetheless it is clear that the L_∞ norm of the solution after some strong initial increase appears to reach a plateau, probably corresponding to some asymptotically solitonic solution. Though the energy of the initial data is negative, there is no reason to assume that there will be blow-up in this case. Since there is sufficient resolution in Fourier space (also shown in Fig. 7) and since the computed energy is conserved to the order of 10^{-12} , the numerical evidence for this is quite strong.

To test further whether the humps in Fig. 6 are related to solitons, we fit the solitonic solutions constructed numerically in the previous subsection to the humps at the final computed time. To this end we determine the locations and the value of the maxima, shift the numerically constructed soliton solution to these values of x and rescale via (39). This leads to Fig. 8. Obviously the final time is not yet fully in the asymptotic regime for the smaller soliton on the left, but the agreement is already very good there. For the larger soliton, the solutions are hardly distinguishable. Thus

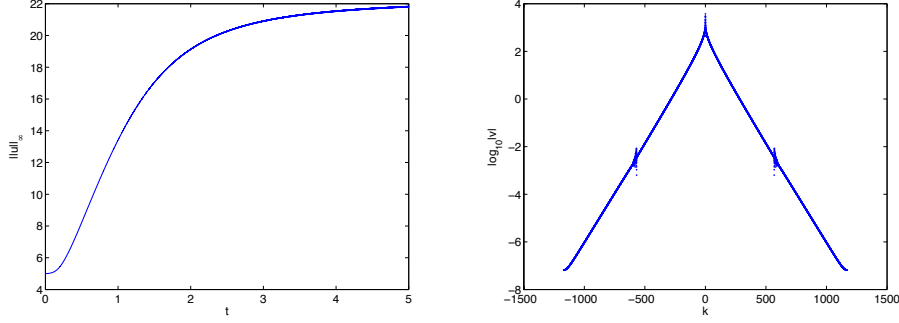


FIGURE 7. L_∞ norm of the solution to the fKdV equation (7) for $\alpha = 0.6$ and the initial data $u_0 = 5\text{sech}^2 x$ in dependence of time on the left, and the modulus of the Fourier coefficients of the solution for $t = 5$ on the right.

it appears that solutions to the fKdV equation decompose for large times into solitons and radiation.

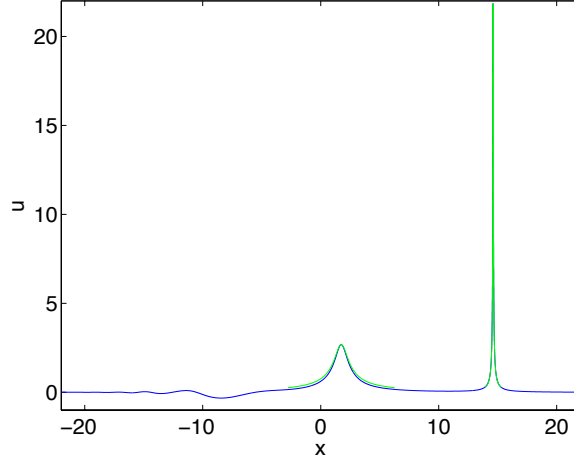


FIGURE 8. Solution to the fKdV equation (7) for $\alpha = 0.6$ and the initial data $u_0 = 5\text{sech}^2 x$ for $t = 5$ in blue, fitted solitons at the humps in green.

There are also no indications for blow-up for the critical case $\alpha = 0.5$ and the initial data $u_0 = \text{sech}^2 x$ which can be seen in Fig. 9 and for which the energy is positive (and thus larger than the soliton energy which is equal to zero) and for which the mass ($M[u_0] = 4/3$) is smaller than the soliton mass $M \sim 3.043$. We use $N = 2^{14}$ Fourier modes for $x \in 10[-\pi, \pi]$ and $N_t = 10^3$ time steps for the computation. The solution is well resolved in Fourier space and the computed energy is conserved to the order of 10^{-12} .

Dispersive oscillations form immediately, and after a short increase the L_∞ norm of the solution appears to decrease monotonically. The initial hump seems to be radiated away, it is below the threshold to form a soliton.

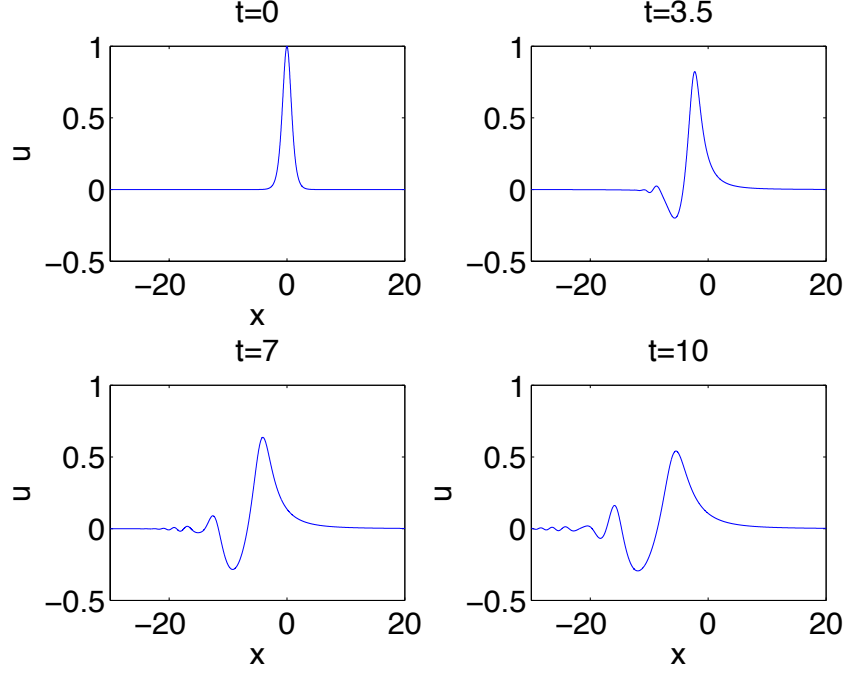


FIGURE 9. Solution to the fKdV equation (7) for $\alpha = 0.5$ and the initial data $u_0 = \text{sech}^2 x$ for several values of t .

The picture changes completely for the same α and the initial data $u_0 = 3\text{sech}^2 x$ for which the energy is negative and for which the mass $M[u_0] = 12$ is larger than the soliton mass. The solution for this case can be seen in Fig. 10. The initial hump gets again laterally compressed and increases in height, a soliton seems to emerge. But this time it appears that the oscillations forming at the same time and propagating to the left cannot compensate the increase in height, the ‘soliton’ seems to be unstable and eventually blows up. We compute with $N = 2^{16}$ Fourier modes for $x \in 20[-\pi, \pi]$ and $N_t = 10^4$ time steps.

We stop the code at $t = 7$ where the computed relative energy drops below 10^{-3} which implies that the solution is no longer reliable for larger times. Note that the time where the code is stopped for this reason is not taken as the blow-up time. The latter is determined below via a fitting to a theoretical blow-up scenario. As can be seen in Fig. 11, the loss of accuracy due to a lack of resolution in Fourier space due to the strongly peaked hump, not to a lack in resolution in time. It is also clear from Fig. 11 that the L_∞ norm of the solution increases monotonically. As in the L_2 critical case for

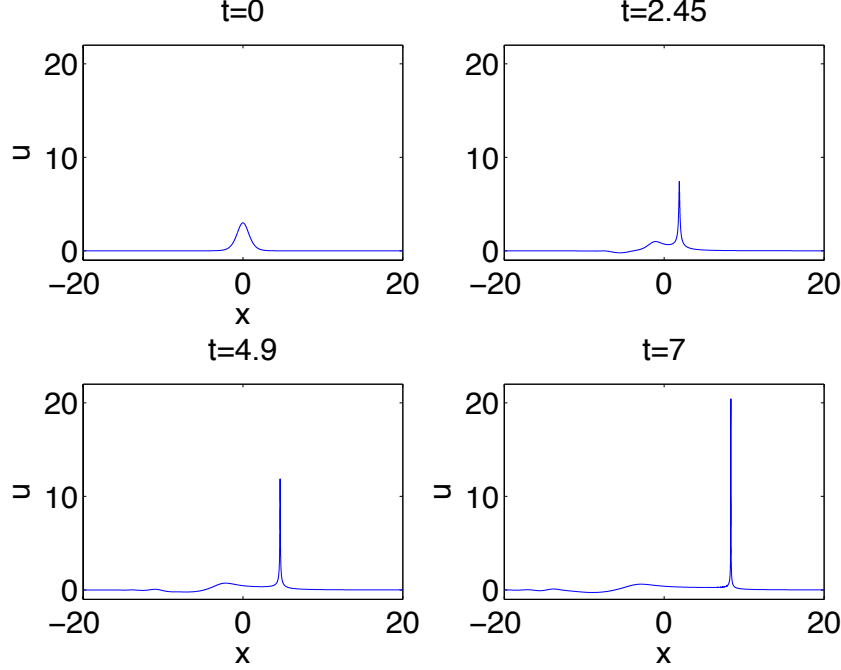


FIGURE 10. Solution to the fKdV equation (7) for $\alpha = 0.5$ and the initial data $u_0 = 3\text{sech}^2 x$ for several values of t .

gKdV in [29], this increase appears to be algebraic in time. The peak which appears to blow up eventually gets more and more compressed laterally, grows in height and propagates faster. Thus it seems to be similar to the blow-up in the L_2 critical case for gKdV, also in the sense that the solution could blow up at x^* with $x^* \rightarrow \infty$.

For t close enough to the blow-up time t^* , it is possible to fit the data to the expected scalings (34) and (35) to characterize the type of blow-up further. The task is to find the range of the values of t where the asymptotic behavior can be already observed whilst still allowing for a large enough interval to have sufficient computed values for the fitting. The problem is that the blow-up time t^* is not known and has to be determined in the process. In [29] it was shown that this can be done with the optimization algorithm [33] distributed with Matlab as *fminsearch*. In Fig. 12 we show the fits for the L_2 norm of u_x and the L_∞ norm of u for $4.1993 < t < 7$. The results of the fitting do not change much if the lower bound is slightly changed. For both quantities the logarithms are fitted to $\kappa_1 \ln(t^* - t) + \kappa_2$. For $\|u\|_\infty$ we find $t^* = 9.8712$, $\kappa_1 = -0.9901$ and $\kappa_2 = 4.0609$, for $\|u_x\|_2^2$ we obtain $t^* = 9.8393$, $\kappa_1 = -3.9785$ and $\kappa_2 = 20.4335$. Thus both fittings are consistent within numerical accuracy, and are compatible with (34) for $\gamma = 1$ which is exactly the value for the L_2 critical gKdV.

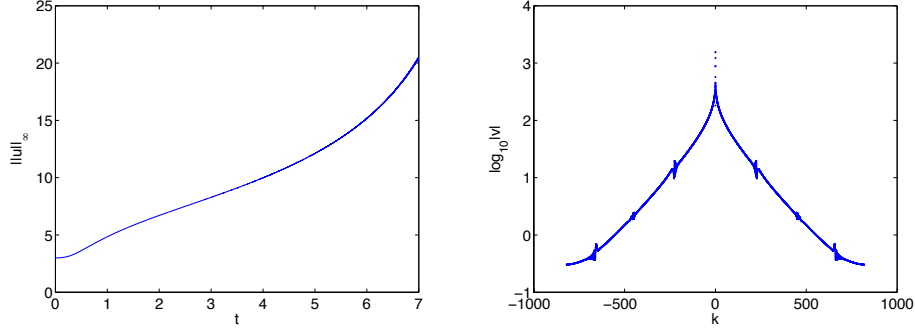


FIGURE 11. L_∞ norm of the solution to the fKdV equation (7) for $\alpha = 0.5$ and the initial data $u_0 = 3\text{sech}^2 x$ in dependence of time on the left, and the modulus of the Fourier coefficients of the solution for $t = 7$ on the right.

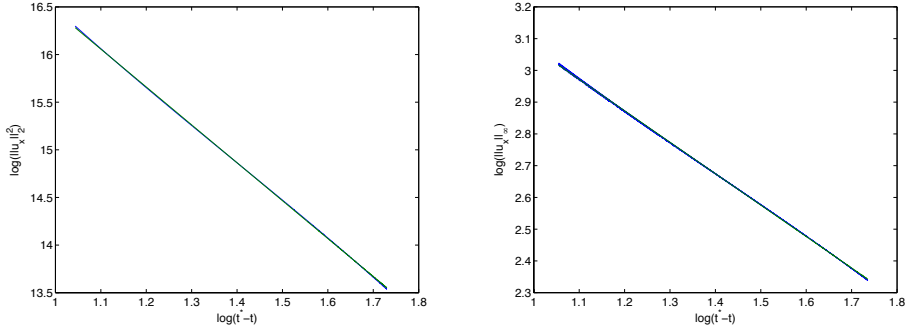


FIGURE 12. L_2 norm of the gradient (left) and L_∞ norm of the solution to the fKdV equation (7) for $\alpha = 0.5$ and the initial data $u_0 = 3\text{sech}^2 x$ (right) for $t > 4.1993$ in blue and the fitted lines $\kappa_1 \ln(t^* - t) + \kappa_2$ in green.

There are, however, more implications from the dynamic rescaling (27). Since the dependence of the norms in Fig. 12 appears to be algebraic in the rescaled time τ , the blow-up profile should be asymptotically given by a rescaled soliton (11). To test this we fit the hump in the last frame of Fig. 10 according to (27) by reading the value of L off from the maximum of the solution. The result of this fitting to the numerically obtained soliton can be seen in Fig. 13. This fitting is analogous to the one for the case $\alpha = 0.6$ in Fig. 8, the difference being that for $\alpha > 0.5$, humps of sufficient size asymptotically approach an exact fKdV soliton, whereas for $\alpha = 0.5$ a hump of sufficient size will simply blow up with a profile of a dynamically rescaled soliton. The good agreement of the fitting indicates that blow-up in the solution to the L_2 critical fKdV equations is indeed given by a

dynamically rescaled soliton. This implies that most of the L_2 norm of the initial data will be asymptotically concentrated in the rescaled soliton.

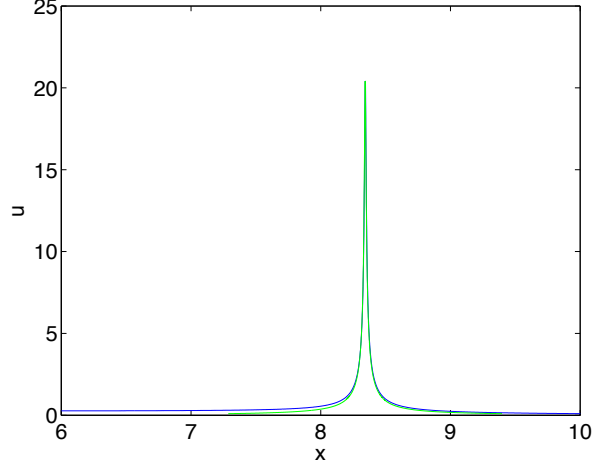


FIGURE 13. Solution to the fKdV equation (7) for $\alpha = 0.5$ and the initial data $u_0 = 3\text{sech}^2 x$ for $t = 7$ in blue and the fitted soliton (11) rescaled according to (27) in green.

Note that it cannot be decided numerically whether energy zero marks a dividing line between radiation and blow-up. We can only state that the solution behaves decisively differently for clearly positive and negative energies. For the L_2 critical case $\alpha = 0.5$, it appears that negative energy (the soliton has vanishing energy) or a mass greater than the soliton mass are as for gKdV with $n = 4$ the criterion for blow-up.

For $1/3 < \alpha < 0.5$, i.e., the L_2 supercritical case, there are certain similarities to the L_2 critical case. For initial data with a mass smaller than the soliton mass, the initial hump just appears to be radiated away as can be seen for $u_0 = \text{sech}^2 x$ and $\alpha = 0.45$ in Fig. 14. The mass of these data $M[u_0] = 4/3$ is clearly smaller than the soliton mass which is roughly 2.375.

In Fig. 15 we show the solution to the fKdV equation for the initial data $u_0 = 3\text{sech}^2 x$ for which the mass is $M[u_0] = 12$ and thus much larger than the soliton mass 2.375. It can be seen that a soliton forms in the evolution of the initial hump which separates from the remainder of the initial data to finally blow up. Visibly the type of blow-up is different from the mass critical case in Fig. 13 since the L_2 norm of the initial data is no longer concentrated in the blow-up profile. This is the same type of behavior known from supercritical blow-up in gKdV equations, see for instance [29].

The code is stopped at $t = 1.86$ since the conservation of the numerically computed energy drops below 10^{-3} . As can be seen in Fig. 16, this is due

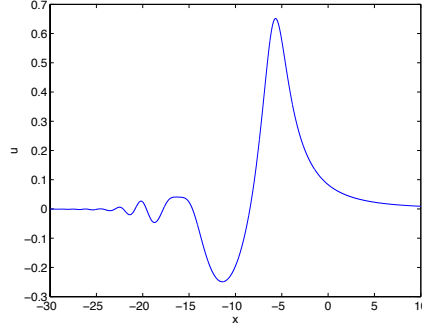


FIGURE 14. Solution to the fKdV equation (7) for $\alpha = 0.45$ for the initial data $u_0 = \text{sech}^2 x$ at $t = 10$.

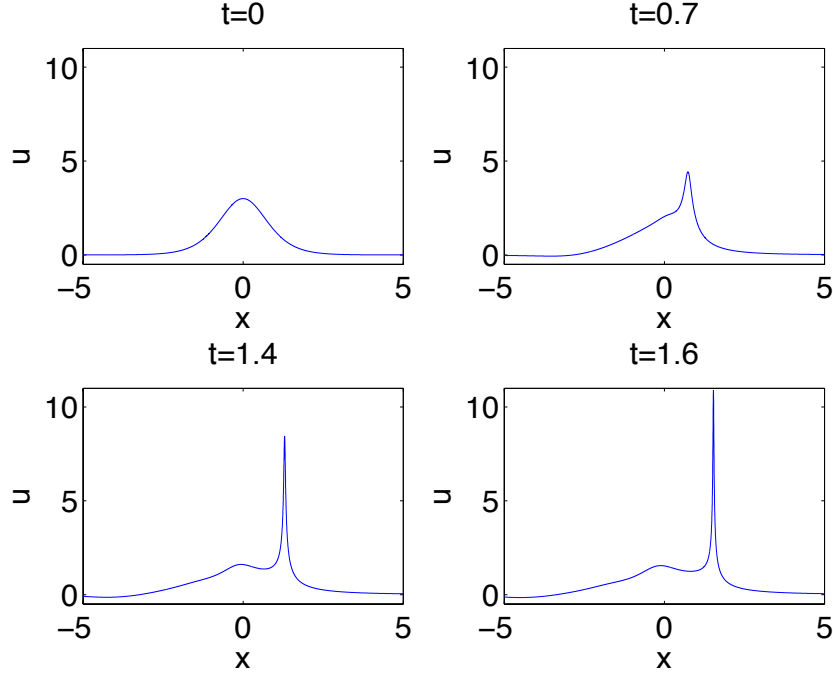


FIGURE 15. Solution to the fKdV equation (7) for $\alpha = 0.45$ for the initial data $u_0 = 3\text{sech}^2 x$ for several values of t .

to a lack of resolution in Fourier space. The L_∞ norm of the solution in the same figure also indicates a blow-up.

As for the L_2 critical case $\alpha = 0.5$ in Fig. 12, we can fit various norms of the solution close to the blow-up to the formulae (34) and (35) which can be seen in Fig. 17. Fitting $\|u_x\|_2^2$ to $\kappa_1 \ln(t^* - t) + \kappa_2$, we find $t^* = 1.9489$, $\kappa_1 = -2.2137$ and $\kappa_2 = 11.7436$, and similarly we get for $\|u\|_\infty$ $t^* = 1.9522$,

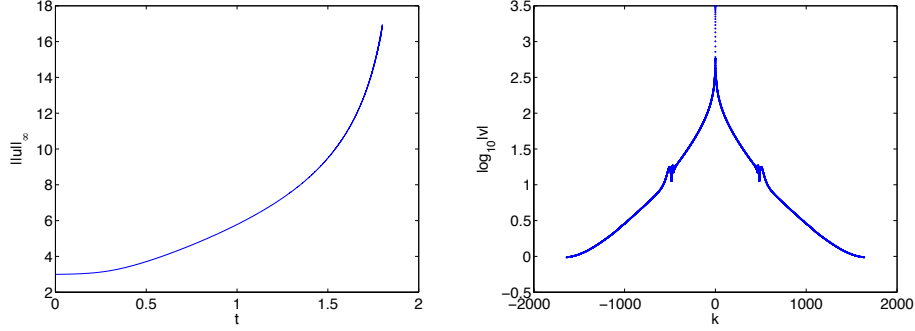


FIGURE 16. L_∞ norm of the solution to the fKdV equation (7) for $\alpha = 0.45$ and the initial data $u_0 = 3\text{sech}^2 x$ in dependence of time on the left, and the modulus of the Fourier coefficients of the solution for $t = 1.86$ on the right.

$\kappa_1 = -0.5231$ and $\kappa_2 = 1.8441$. Thus the fitted values for t^* are consistent and in accordance with the computation. The agreement with expectation is better for the L_∞ norm for κ_1 which should be according to (35) 1.31 and 0.31 respectively.

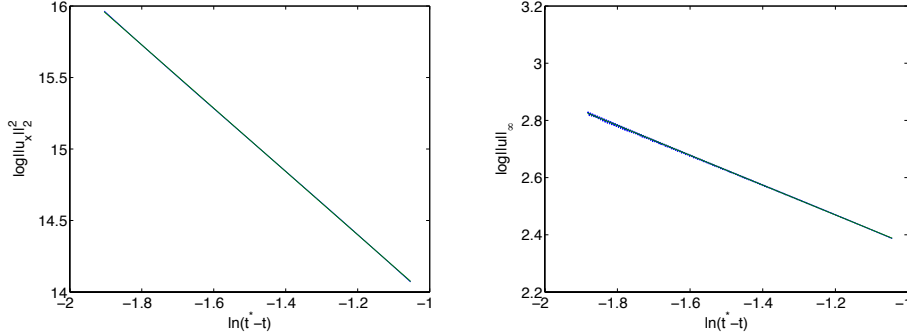


FIGURE 17. L_2 norm of the gradient (left) and L_∞ norm of the solution to the fKdV equation (7) for $\alpha = 0.45$ and the initial data $u_0 = 3\text{sech}^2 x$ (right) for the last 1000 time steps in blue and the fitted lines $\kappa_1 \ln(t^* - t) + \kappa_2$ in green.

The exact criterion for the initial data to lead to a blow-up in finite time is not clear. For $1/3 < \alpha < 1/2$ it could be related to the mass or energy of the soliton. But since there are no solitons for $\alpha \leq 1/3$, the soliton for the given value of α cannot provide a criterion unless there is always blow-up. However, this is not the case for smaller initial data as can be seen for instance in Fig. 18 where we show the solution to the fKdV equation for the initial data $u_0 = 0.1\text{sech}^2 x$. The solution will be just radiated away to infinity for large times even if $\alpha < 1/3$. The computation is carried out with $N = 2^{14}$ Fourier modes for $x \in 20[-\pi, \pi]$ with $N_t = 10^4$ time

steps for $t \leq 20$. It can be seen in the same figure that the L_∞ norm of the solution is monotonically decreasing. Thus there is no indication of blow-up for initial data with small enough mass. Obviously there can be globally regular solution for all t in this case, which is in strong contrast with the Burgers equation for which any localized initial data leads to a shock formation.

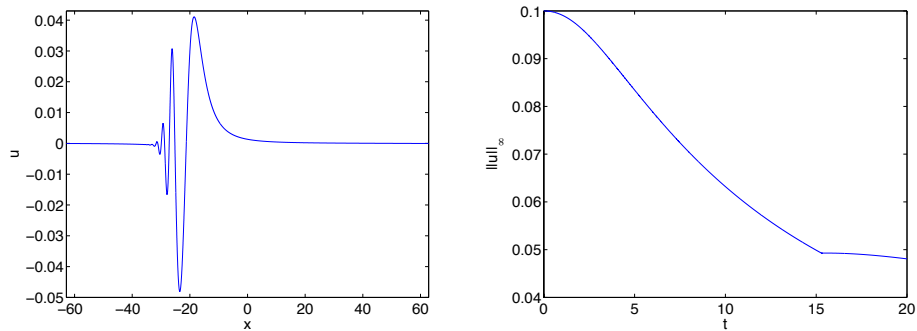


FIGURE 18. Solution to the fKdV equation (7) for $\alpha = 0.2$ and the initial data $u_0 = 0.1\text{sech}^2 x$ (right) for $t = 20$ on the left, and the L_∞ norm of the solution in dependence of t on the right.

The situation is different for larger data. For $\alpha = 0.2$, the energy of the initial data $u_0 = \text{sech}^2 x$ is positive, but there seems to be a much more pronounced blow-up than in the blow-up cases above as can be seen in Fig. 19. In this case there are almost no dispersive oscillations visible since the dispersion is much weaker, and the whole initial hump seems to be increasingly peaked. Obviously there can be no soliton forming which then blows up. But there is a rapid increase in the L_∞ norm at $t = 3.045$ where the code ceases to converge. Thus for $\alpha < 1/3$, blow-up is observed also for initial data with positive energy. Note the difference in the type of blow-up in the energy supercritical case here and for $\alpha = 0.45$ in Fig. 15. There a soliton forms which is unstable against blow-up. Here the solution follows initially the pattern of a solution to the Burgers' equation, a steepening almost leading to a shock. But instead of reaching a point of gradient catastrophe, the maximum of the solution appears to turn into an L_∞ blow-up.

This rapid increase in the L_∞ norm is even more visible in Fig. 20. It can be also seen in this figure that the failure of the code to converge is due to a lack of resolution in Fourier space (the computed relative energy is still conserved to the order of 10^{-10}).

As for the above blow-up cases, we can fit various norms of the solution close to the blow-up to the formulae (34) and (35). The rapid divergence of the norms indicates already an exponential (in the rescaled time τ) blow-up, and this is confirmed by the fitting procedure. However, such an exponential

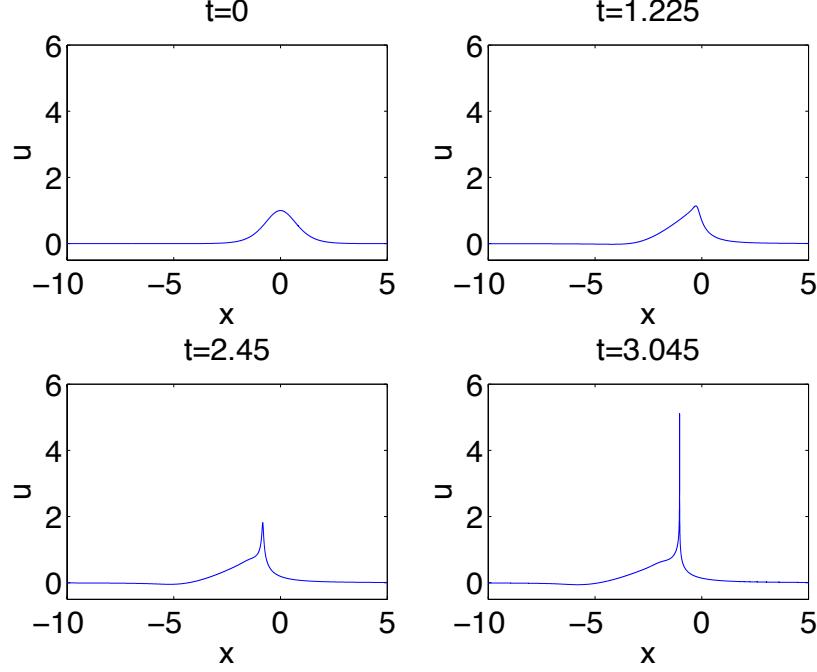


FIGURE 19. Solution to the fKdV equation (7) for $\alpha = 0.2$ and the initial data $u_0 = \text{sech}^2 x$ for several values of t .

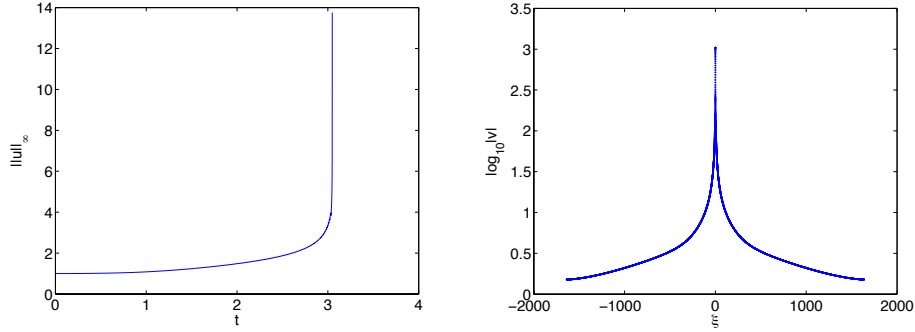


FIGURE 20. L_∞ norm of the solution to the fKdV equation (7) for $\alpha = 0.2$ and the initial data $u_0 = \text{sech}^2 x$ in dependence of time on the left, and the modulus of the Fourier coefficients of the solution for $t = 3.045$ on the right.

behavior implies a less good fitting since it will be dominant only very close to the blow-up where the code is no longer fully reliable. Thus we fit on a larger interval, $2.4497 < t < 3.045$ and note that the fitting parameters get closer to the theoretically expected ones if the lower bound is increased. It

can be seen in Fig. 21 that the fitting is very sensitive to the fitted time t^* , and that it is problematic for $t \sim t^*$. Fitting $\|u_x\|_2^2$ to $\kappa_1 \ln(t^* - t) + \kappa_2$, we find $t^* = 3.0490$, $\kappa_1 = -1.2552$ and $\kappa_2 = 8.4845$, and similarly we get for $\|u\|_\infty$ $t^* = 3.0489$, $\kappa_1 = -0.2245$ and $\kappa_2 = 0.5210$. Thus the fitted values for t^* are consistent and in accordance with the computation. This also applies within numerical precision to the values of κ_1 which should be according to (35) $7/6$ and $1/6$ respectively.

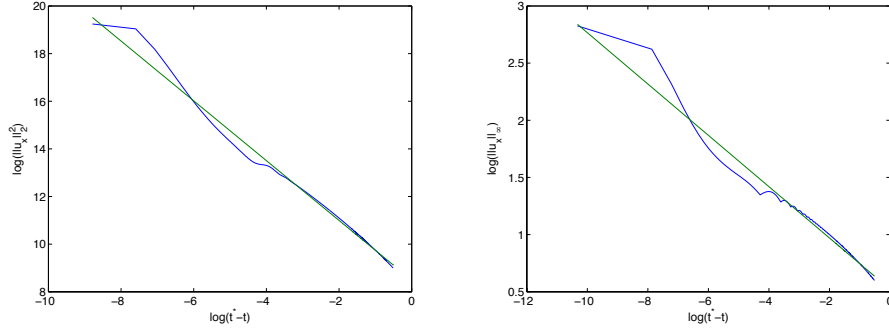


FIGURE 21. L_2 norm of the gradient (left) and L_∞ norm of the solution to the fKdV equation (7) for $\alpha = 0.2$ and the initial data $u_0 = \text{sech}^2 x$ (right) for $t > 2.4497$ in blue and the fitted lines $\kappa_1 \ln(t^* - t) + \kappa_2$ in green.

Remark 1. In the cases with blow-up, we can test whether the Fourier coefficients can be fitted to the asymptotic formula (36) which should indicate the formation of a singularity on the real axis via the vanishing of the parameter δ . For the example of an L_2 critical blow-up in Fig. 11 we get $\delta = 0.007$ and $\mu + 1 = 0.36$. This indicates in accordance with the fitting of the norms in Fig. 13 that the blow-up is not fully reached. The exact value of μ is probably not reliable (it is less accurate since the fitting to an exponential is less prone to errors than to a linear dependence), but its sign indicates that the singularity is a pole, in accordance with what was found for the L_∞ norm of the solution. For the L_2 supercritical blow-up in Fig. 15, we find $\mu + 1 = 0.6535$ and $\delta = 0.0023$, where μ is once more less reliable. This indicates that we are shortly before the blow-up, and that this is again an L_∞ blow-up. For the energy supercritical blow-up in Fig. 20 we find $\delta = -0.003$ and $\mu + 1 = 0.8077$. This indicates in accordance with the fitting of the norms in Fig. 21 that blow-up is indeed reached. The divergence of the solution appears to be proportional to $|x - x^*|^{-\alpha}$.

We summarize the numerical findings in this subsection in the following

Conjecture 1. Consider smooth initial data $u_0 \in L_2(\mathbb{R})$ with a single hump. Then for

- $\alpha > 0.5$: solutions to the fKdV equations with the initial data u_0 stay smooth for all t . For large t they decompose asymptotically into solitons and radiation.
- $0 < \alpha \leq 0.5$: solutions to the fKdV equations with initial data u_0 of sufficiently small, but non-zero mass stay smooth for all t .
- $\alpha = 0.5$: solutions to the fKdV equations with the initial data u_0 with negative energy and mass larger than the soliton mass blow up at finite time t^* and infinite x^* . The type of the blow-up for $t \nearrow t^*$ is characterized by

$$(42) \quad u(x, t) \sim \frac{1}{\sqrt{L(t)}} Q_1 \left(\frac{x - x_m}{L(t)} \right), \quad L = c_0(t^* - t),$$

where c_0 is a constant, and where Q_1 is the solitary wave solution (11) for $c = 1$. In addition one has

$$(43) \quad \|u_x\|_2 \sim \frac{1}{L^2(t)}.$$

- $1/3 < \alpha < 0.5$: solutions to the fKdV equations with the initial data u_0 and sufficiently large L_2 norm blow up at finite time t^* and finite $x = x^*$. A soliton-type hump separates from the initial hump and eventually blows up. The type of the blow-up for $t \nearrow t^*$ is characterized by

$$(44) \quad u(x, t) \sim \frac{1}{L^\alpha(t)} U \left(\frac{x - x_m}{L(t)} \right), \quad L = c_1(t^* - t)^{\frac{1}{1+\alpha}},$$

where c_1 is a constant, and where U is a solution of equation (32) vanishing for $|y| \rightarrow \infty$ (if such a solution exists). In addition one has

$$(45) \quad \|u_x\|_2 \sim \frac{1}{L^{2\alpha+1}(t)}.$$

- $0 < \alpha < 1/3$: solutions to the fKdV equations with the initial data u_0 and sufficiently large L_2 norm blow up at finite time t^* and finite $x = x^*$. The nature of blow-up is different from the previous one since no solitary waves exist in this case, the maximum of the initial hump evolves directly into a blow-up. Thus the blow-up seems to be different from that occurring in the supercritical gKdV equation (1) when $p > 4$. But the blow-up profile appears to be still given by (44).

3.4. Numerical study of fractionary BBM equations. In this subsection we study the behavior of solutions to the fractionary BBM (fBBM) equation (12). We consider as before initial data of the form $u_0 = \beta \text{sech}^2 x$ with β a real constant. We find that for $\alpha > 1/3$, initial data of sufficient mass asymptotically decompose into solitons. For $\alpha \leq 1/3$, such data lead to a blow-up in the form of a cusp at which the L_∞ norm of the solution stays finite.

We find a similar behavior of the solutions for $1/3 < \alpha \leq 1$. For $\alpha = 0.5$ and $\beta = 10$ we use $N = 2^{14}$ Fourier modes for $x \in 20[-\pi, \pi]$ and $N_t = 2 \cdot 10^4$ time steps for $t \leq 10$ to obtain the solution shown in Fig. 22. It can be seen that the initial hump splits into several more strongly peaked humps which move like solitons, i.e., without changing their shape with essentially constant speed. This is similar to what was observed for fKdV solutions for $\alpha > 1/2$. For large t the solutions appear to be given by solitons and radiation.

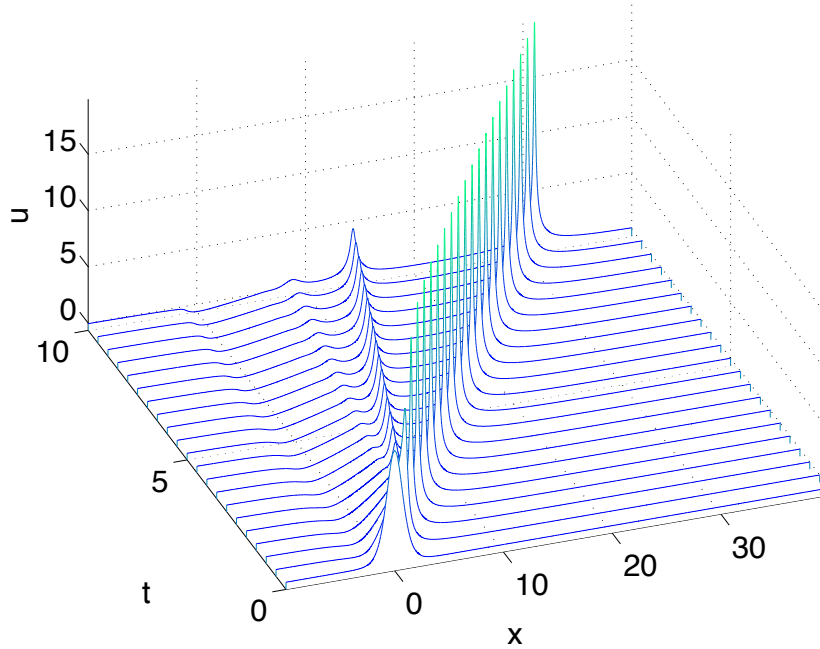


FIGURE 22. Solution to the fBBM equation (12) for $\alpha = 0.5$ and the initial data $u_0 = 10\text{sech}^2 x$ in dependence of x and t .

The computation is carried out with a relative conservation of the computed energy of the order of 10^{-12} . In Fig. 23 it can be seen that the solution is well resolved in Fourier space. The L_∞ norm of the solution confirms the ‘solitonic’ appearance. After an initial increase of the norm, it stays essentially constant. The small oscillations are due to radiation propagating to the left which reenters the computational domain on the right because of the periodic boundary conditions.

There is no indication of blow-up in this case, the solutions appears to be globally smooth in time. This does not change for initial data with larger L_2 norm and energy as can be seen in Fig. 24, where the solution for $u_0 = 20\text{sech}^2 x$ is shown at $t = 10$. In this case the humps into which the initial data decompose have a larger maximum and propagate faster,

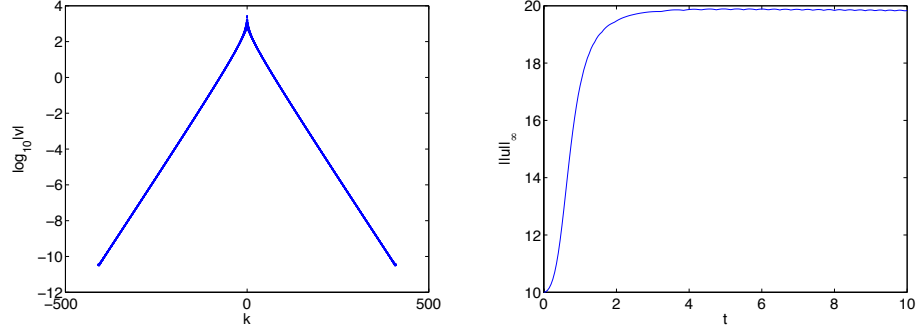


FIGURE 23. Solution to the fBBM equation (12) for $\alpha = 0.5$ for the initial data $u_0 = 10\text{sech}^2 x$ at $t = 10$; on the left the Fourier coefficients, on the right the L_∞ norm in dependence of time.

but there is again no indication of blow-up. We show in Fig. 24 the fitting of the humps to rescaled (according to (39) and (38)) solitons. It can be seen that the largest and left most hump is almost indistinguishable from the soliton, whereas the smallest fitted hump is not yet in the asymptotic regime. Nonetheless the good agreement of the fitting to solitons indicates that the solution asymptotically for large t decomposes into solitons and radiation. Note that this implies that the solitons are stable also for $\alpha \leq 1/2$ for fBBM in contrast to fKdV.

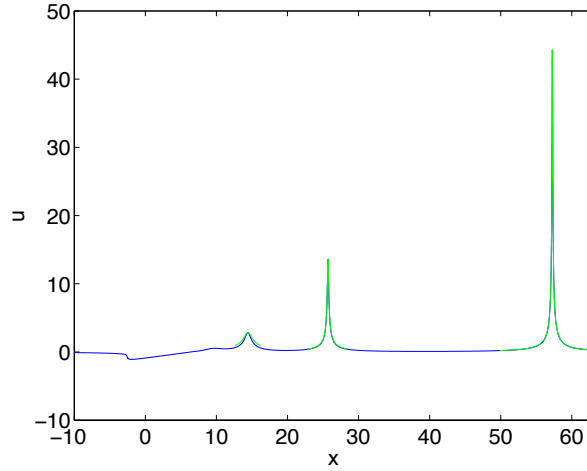


FIGURE 24. Solution to the fBBM equation (12) for $\alpha = 0.5$ and the initial data $u_0 = 20\text{sech}^2 x$ for $t = 10$ in blue, and fitted solitons (11) rescaled according to (39) and (38) in green.

The situation is less clear for $\alpha < 1/3$. We study the solution for $\alpha = 0.2$ and the initial data $u_0 = \text{sech}^2 x$ with $N = 2^{16}$ modes for $x \in 3[-\pi, \pi]$ with

$N_t = 2 * 10^4$ time steps for $t \leq 6$. At $t = 5.85$ the relative computed energy drops below 10^{-3} at which point the code is stopped since the solution is no longer reliable. In Fig. 25 we show the solution for several values of t .

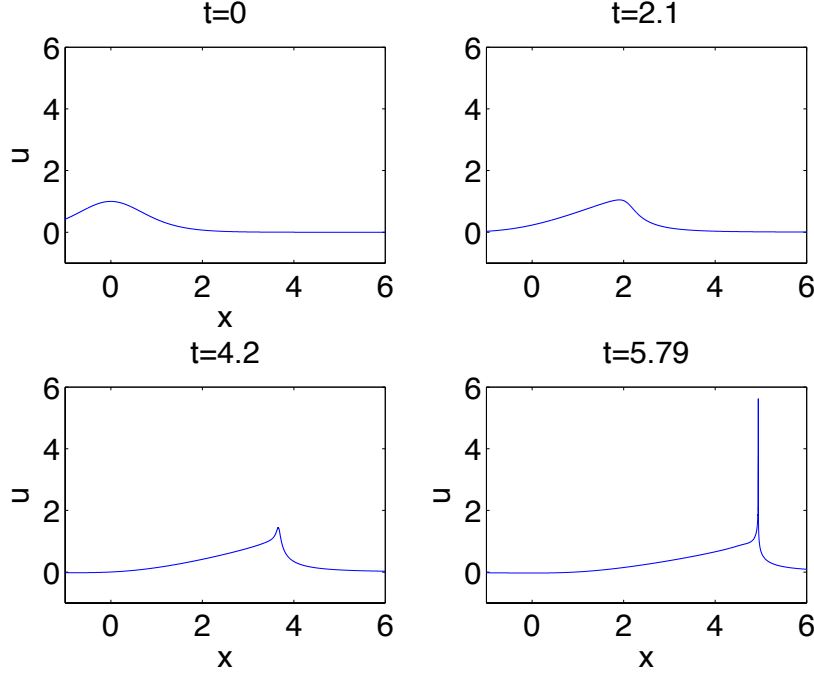


FIGURE 25. Solution to the fBBM equation (12) for $\alpha = 0.2$ and the initial data $u_0 = \text{sech}^2 x$ for several values of t .

The solution appears to have a blow-up in this case, but the type of the formed singularity is not obvious. The Fourier coefficients in Fig. 26 indicate a lack of resolution at $t = 5.85$. The L_∞ norm in the same figure also appears to diverge. If we rerun the code in this case with higher resolution in space and time, we get within numerical precision the same behavior which indicates that this is indeed a blow-up.

A fitting of the Fourier coefficients at the last computed time according to the asymptotic formula (36) yields $\delta = -0.003$ and $\mu + 1 = 1.21$. The value of δ indicates that a singularity has formed. But there seems to be no L_∞ blow-up in this case, but the formation of a cusp of the form $|x - x^*|^\alpha$. This is in clear contrast to corresponding fKdV examples studied in the previous subsection where the blow-up was proportional to $|x - x^*|^{-\alpha}$, i.e., an L_∞ blow-up in contrast to the gradient catastrophe here. Recall that the break-up in the Burgers solution is proportional to $(x - x_c)^{1/3}$.

This result is confirmed qualitatively by a study of the L_∞ norm of the solution and the L_2 norm of the gradient as for fKdV in the previous subsection. We take the time where the singularity appears on the real axis as

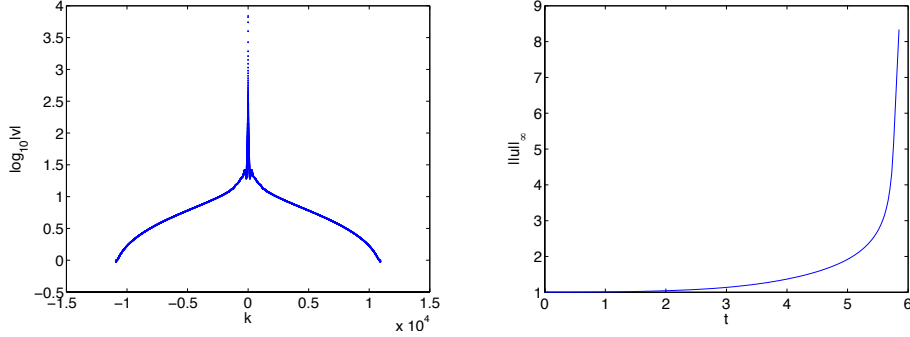


FIGURE 26. Solution to the fBBM equation (12) for $\alpha = 0.2$ for the initial data $u_0 = \text{sech}^2 x$ at $t = 5.85$; on the left the Fourier coefficients, on the right the L_∞ norm in dependence of time.

the blow-up time and study the dependence of the logarithms of the norms on $\ln(t^* - t)$. In both cases there is no linear dependence as in the fKdV case. Instead the L_∞ norm of u seems to approach a constant value in accordance with the expected cusp from the asymptotic behavior of the Fourier coefficients.

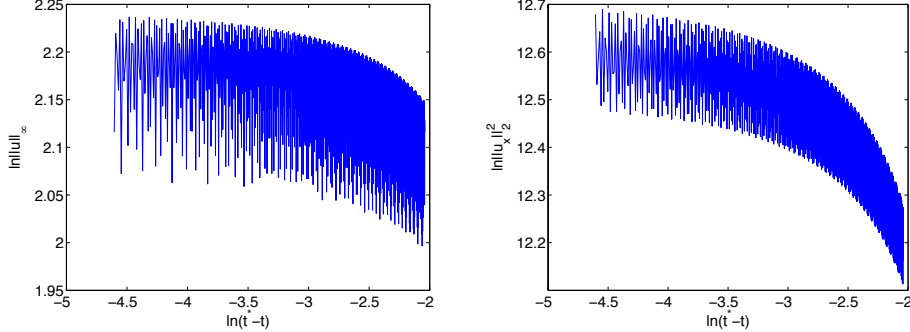


FIGURE 27. Norms of the solution to the fBBM equation (12) for $\alpha = 0.2$ for the initial data $u_0 = \text{sech}^2 x$ at $t = 5.85$; on the left the L_∞ norm of u , on the right the L_2 norm of u_x .

Note that the blow-up in fBBM appears for much later times than the blow-up for the same initial data and the same α for fKdV in Fig. 19. In both cases the time is larger than the breakup time of the solution for the Burgers equation for these initial data, see (50), which is in this case $t_c \sim 1.299$.

For the same α and smaller β , the initial data appear to be just radiated away as can be seen in Fig. 28 for $t = 100 \gg t_c$, where $t_c \sim 12.99$ is the critical time of Burgers solution for the same initial data. The L_∞ norm in the same figure decreases monotonically until the oscillations in the solution set in.

We summarize the numerical findings in this subsection in the following

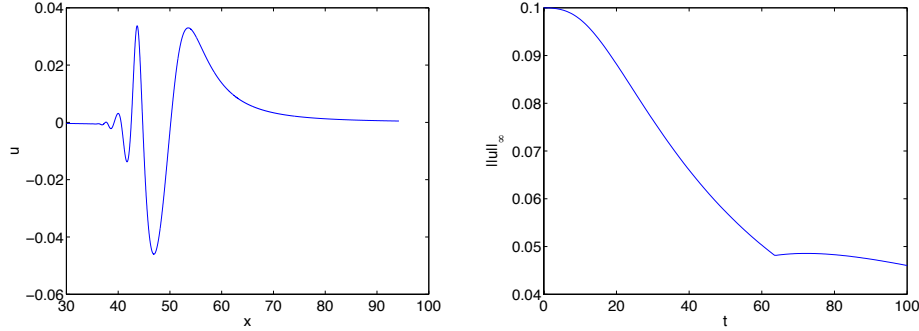


FIGURE 28. Solution to the fBBM equation (12) for $\alpha = 0.2$ for the initial data $u_0 = 0.1\text{sech}^2 x$ at $t = 10$; on left the solution for $t = 100$, on the right the L_∞ norm in dependence of time.

Conjecture 2. Consider smooth initial data $u_0 \in L_2(\mathbb{R})$ with a single hump. Then for

- $\alpha > 1/3$: solutions to the fBBM equations with the initial data u_0 stay smooth for all t . For large t they decompose asymptotically into solitons and radiation.
- $0 < \alpha \leq 1/3$: solutions to the fKdV equations with the initial data u_0 and sufficiently large L_2 norm form a cusp of the form $|x - x^*|^\alpha$ at finite time t^* and finite $x = x^*$. Solutions with sufficiently small initial data are global.
- The fBBM solitons (11) are stable for $\alpha > 1/3$.

Remark 2. We note here a strong contrast between the gKdV equation (1) and the generalized BBM equation

$$(46) \quad u_t + u_x + u^p u_x - u_{xxt} = 0.$$

For both (1) and (46), the critical exponent for the stability of solitary waves is $p = 4$, though the explanation for instability when $p \geq 4$ is different since no blow-up occurs for (46), whatever p .

For the fKdV and fBBM equations the critical exponents seem to be respectively $\alpha = 1/2$ and $\alpha = 1/3$.

3.5. Numerical study of the Whitham equation. In this subsection, we will study numerically solutions to the Whitham equation (4) and for fKdV with negative α , in particular $\alpha = -1/2$ which should show the same dispersion as the Whitham equation for the high wavenumbers. We consider again initial data of the form $u_0 = \beta \text{sech}^2 x$. However this time we will also consider negative β since these are the initial data where the Whitham equation could develop solitons (see [11]). For negative initial data, the solution will propagate to the left, and a gradient catastrophe of the Burgers solution is also expected to the left of the hump for such data. We find that the dispersion is strong enough for initial data of small norm to radiate the

initial hump away to infinity. However, solutions for larger values of $|\beta|$ show a hyperbolic blow-up for $t^* > t_c$, where t_c is the time of shock formation of the Burgers solution for the same initial data. For positive initial data, a cusp formation appears possible even for $t < t_c$.

We first study initial data $u_0 = -0.1\text{sech}^2 x$. The break-up time of the Burgers solution for these data is $t_c \sim 12.99$. We use $N = 2^{14}$ Fourier modes for $x \in 20[-\pi, \pi]$ with $N_t = 10^4$ time steps for $t < 20$, i.e., larger than t_c . It can be seen in Fig. 29 that both the solution to the Whitham and the fKdV equation for $\alpha = -1/2$ appear to be simply radiated away to infinity. The more sophisticated dispersion leads to more oscillations for the solution to the Whitham equation.

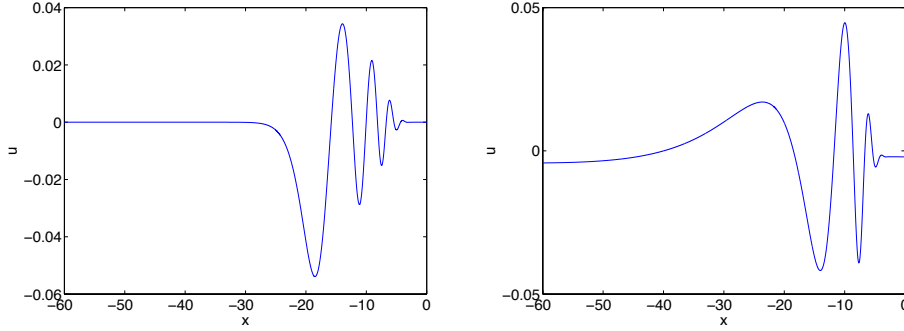


FIGURE 29. Solution to the Whitham equation (4) for the initial data $u_0 = -0.1\text{sech}^2 x$ at $t = 20$ on left, and the solution to the fKdV equation for $\alpha = -1/2$ for the same initial data at the same time on the right.

There is no indication for a blow-up in this case as is even more obvious from various norms of the solution. In Fig. 30 we show the L_∞ norm of the Whitham solution and the L_2 norm of the gradient of the solution, which are both monotonically decreasing. The corresponding norms of the fKdV solution in Fig. 29 are not presented here, but are also decreasing.

The picture changes if we consider the same situation for the initial data $u_0 = \text{sech}^2 x$. We use $N = 2^{16}$ Fourier modes for $x \in 5[-\pi, \pi]$ and $N_t = 20000$ time steps for $t < 2.1$ (the break-up time of the Burgers solution in this case is $t_c \sim 1.299$). Note that for the high wavenumbers, both the Whitham and the fKdV equation with $\alpha = -1/2$ show a weaker dispersion ($\propto |k|^{1/2}$) than a first order derivative which could be eliminated via a Galilean transformation. As can be seen in Fig. 31, the solution shows for early times the same behavior as the corresponding Burgers solution, a steepening of one front of the solution with an increasing gradient. At a given point the maximum of the solution turns into a cusp forming for $t > t_c$. This is a different type of singularity as observed in the Burgers shock where the inflection point becomes singular. The forming of the cusp

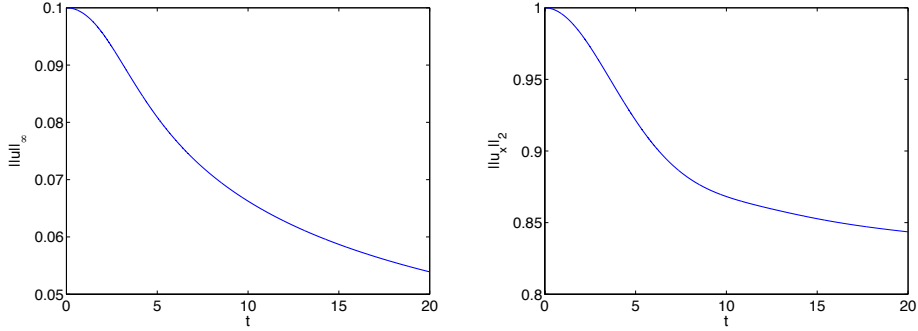


FIGURE 30. L_∞ norm of the Whitham solution of Fig. 29 in dependence of time on the left, and the corresponding L_2 norm of u_x (normalized to 1 for $t = 0$) on the right.

leads to an increase of the modulus of the Fourier coefficients for the high wavenumbers. We fit the Fourier coefficients to the formula (36). The code is stopped when $\delta \sim 10^{-6}$, where the numerically computed energy at the last shown time in Fig. 31 is still of the order of 10^{-10} . We find $\mu + 1 \sim 1.36$ which indicates a cusp of the form $u \sim |x - x^*|^{1/3}$, i.e., the same one would find for the Burgers shock. Note that no solitary wave seems to be forming in the solution, but the existence proof in [11] does not provide an estimate for the velocity of the solitary wave which is obtained as a Lagrange multiplier.

The Fourier coefficients at the last shown time in Fig. 31 can be seen in Fig. 32. The solution to the fKdV equation for $\alpha = -1/2$ for the same initial data can be seen in the same figure. Here the solution becomes singular (as indicated by a vanishing for the parameter δ in (36)) at a later time, and we find $\mu + 1 \sim 1.515$. Thus there seem to be the same reasons for the singularity formation in solutions to the Whitham and the fKdV equation for $\alpha = -1/2$.

The type of the singularity is also confirmed by the norms of the solution to the Whitham equation (the corresponding norms for the fKdV solution are very similar and thus not shown) in Fig. 33. Both norms are only moderately increasing at the time t^* .

Although there are no solitons in this case, we also study positive initial data to allow for a comparison with the results for fKdV in the previous subsections. Initial data as $u_0 = 0.1 \text{sech}^2 x$ of small mass again appear to be just radiated away for both the Whitham equation and fKdV with $\alpha = -1/2$ as can be seen in Fig. 34. There is also no indication for a blow-up in this case from the L_∞ norm of u or the L_2 norm of u_x .

Initial data with more mass as $u_0 = \text{sech}^2 x$ lead to a behavior different from both the small mass and the blow-up case for negative initial data. We use $N = 2^{16}$ Fourier modes for $x \in 5[-\pi, \pi]$ and $N_t = 20000$ time steps for $t < 1.3$ (the break-up time of the Burgers solution in this case is $t_c \sim 1.299$). This is the only time in this paper that the code breaks

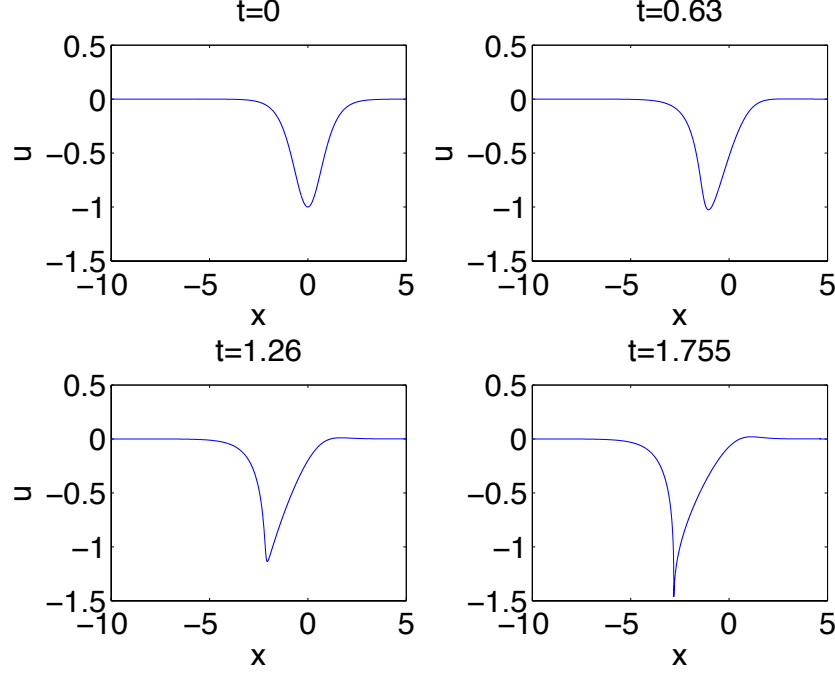


FIGURE 31. Solution to the Whitham equation (4) for the initial data $u_0 = -\text{sech}^2 x$ for several values of t .

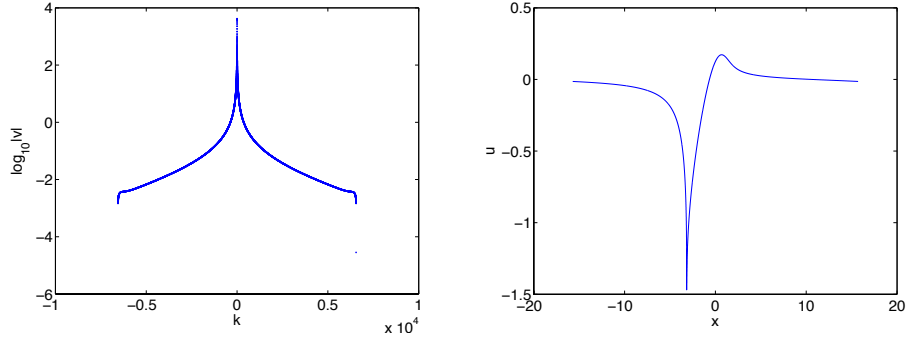


FIGURE 32. Modulus of the Fourier coefficients of the solution to the Whitham equation for the initial data $u_0 = -\text{sech}^2 x$ for $t = 1.764$ on the left, and the solution for the fKdV equation for the same initial data for $t = 2.001$ on the right.

due to *aliasing errors*, i.e., due to a growing of the Fourier modes for the high wave numbers. This can be understood in a hand-waving manner as follows: for the high wavenumbers, both the Whitham and the fKdV equation with $\alpha = -1/2$ show a weaker dispersion ($\propto |k|^{1/2}$) than a first order derivative. As can be seen in Fig. 31, the solution shows for early

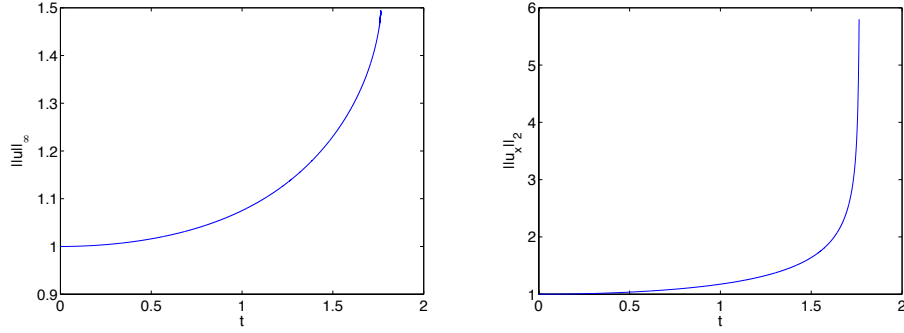


FIGURE 33. L^∞ norm of the Whitham solution of Fig. 31 in dependence of time on the left, and the corresponding L_2 norm of u_x on the right.

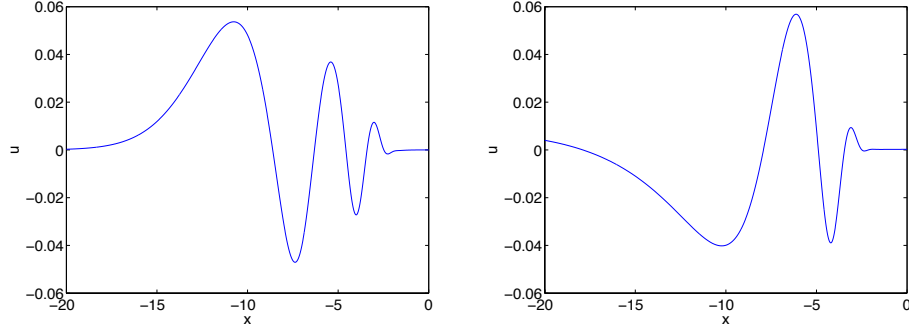


FIGURE 34. Solution to the Whitham equation (4) for the initial data $u_0 = 0.1\text{sech}^2 x$ at $t = 13$ on left, and the solution to the fKdV equation for $\alpha = -1/2$ for the same initial data at the same time on the right.

times the same behavior as the corresponding Burgers solution, a steepening of one front of the solution with an increasing gradient. At a given point there is a cusp forming for $t < t_c$ to the right of the point where the point of gradient catastrophe of the Burgers solution would appear. This leads to an increase of the modulus of the Fourier coefficients for the high wavenumbers. The weak dispersion together with unavoidable numerical errors leads to an amplification of this phenomenon which would eventually break the code. To address these aliasing problems we use dealiasing according to the 2/3 rule, i.e., we put the Fourier coefficients corresponding to the 1/3 highest wavenumbers equal to zero. We fit the remaining Fourier coefficients to the formula (36). The code is stopped when $\delta \sim 10^{-6}$, where the numerically computed energy at the last shown time in Fig. 35 is still of the order of 10^{-11} . We find $\mu + 1 \sim 1.516$ which indicates a cusp of the form $u \sim |x - x^*|^{1/2}$.

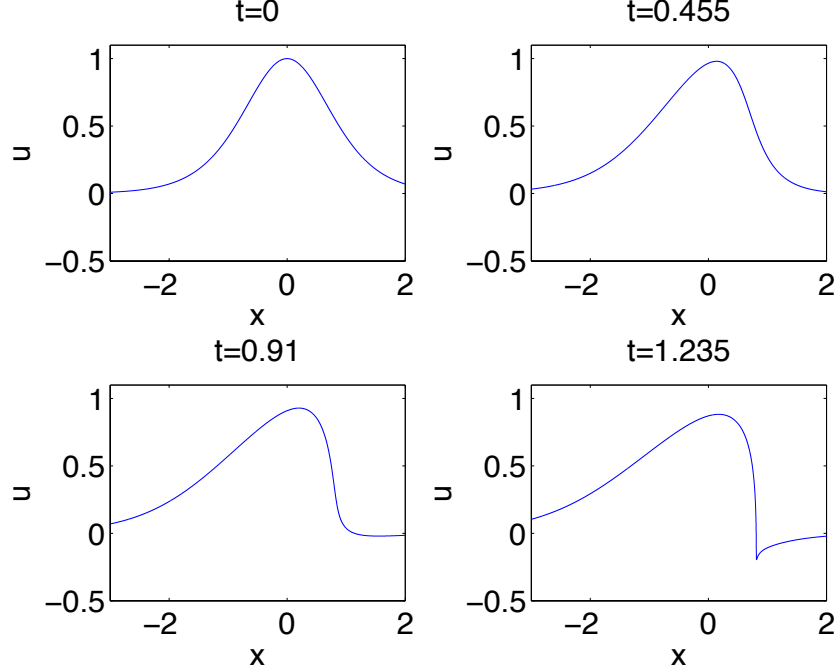


FIGURE 35. Solution to the Whitham equation (4) for the initial data $u_0 = \text{sech}^2 x$ for several values of t .

The Fourier coefficients at the last shown time in Fig. 31 can be seen in Fig. 36. The dealiasing is clearly visible. The solution to the fKdV equation for $\alpha = -1/2$ for the same initial data can be seen in the same figure. Here the solution becomes singular (as indicated by a vanishing for the parameter δ in (36)) at an even earlier time, and we find $\mu + 1 \sim 1.515$. Thus there seem to be the same reasons for the singularity formation in solutions to the Whitham and the fKdV equation for $\alpha = -1/2$ also for positive initial data.

The type of the singularity is once more confirmed by the norms of the solution to the Whitham equation (the corresponding norms for the fKdV solution are very similar and thus not shown) in Fig. 37. The L_∞ norm of the solution is monotonically increasing, the L_2 norm of the gradient has a blow-up. But as the Fourier coefficients indicate, this is not a cubic but a square root singularity in this case.

The results of this subsection can be summarized in the following

Conjecture 3. *Consider smooth initial data $u_0 \in L_2(\mathbb{R})$ with a single negative hump. Then*

- *solutions to the Whitham equation (4) and to fKdV equations with $-1 < \alpha < 0$ for initial data u_0 of sufficiently small mass stay smooth for all t and will be radiated away.*

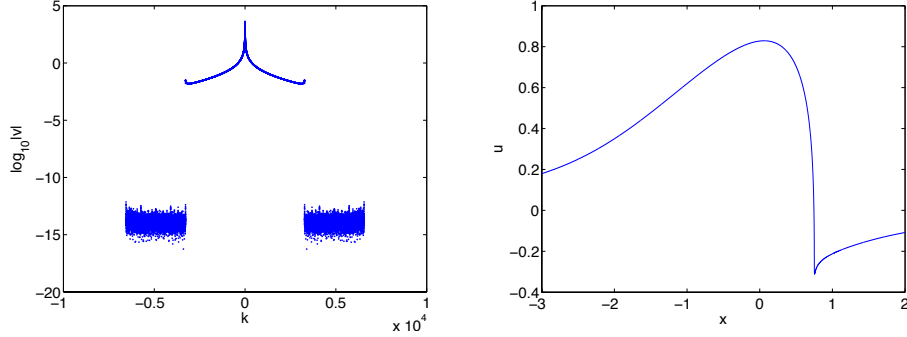


FIGURE 36. Modulus of the Fourier coefficients of the solution to the Whitham equation for the initial data $u_0 = \text{sech}^2 x$ for $t = 1.235$ on the left, and the solution for the fKdV equation for the same initial data for $t = 1.2109$ on the right.

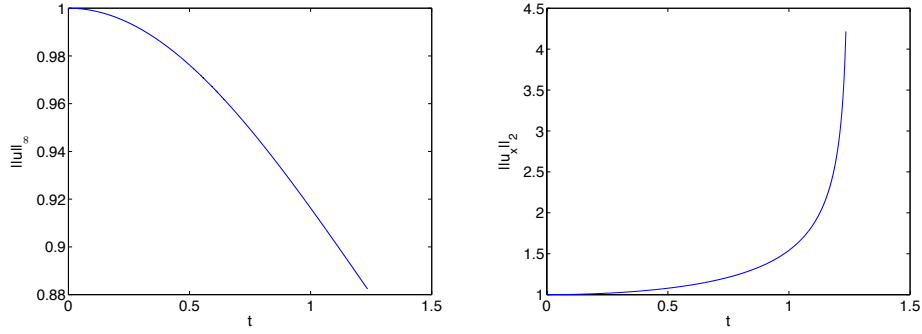


FIGURE 37. L^∞ norm of the Whitham solution of Fig. 31 in dependence of time on the left, and the corresponding L_2 norm of u_x on the right.

- solutions to the Whitham equation (4) and to the fKdV equation with $\alpha = -1/2$ for negative initial data u_0 of sufficiently large mass will develop a cusp at $t^* > t_c$ of the form $|x - x^*|^{1/3}$. The sup norm of the solution remains bounded at the blow-up point.
- solutions to the Whitham equation (4) and to the fKdV equation with $\alpha = -1/2$ for positive initial data u_0 of sufficiently large norm mass will develop a cusp at $t^* < t_c$ of the form $|x - x^*|^{1/2}$.

3.6. Large time behavior. In this subsection we study the long time behavior of solutions to the fKdV (15) and fBBM equation (20) in the case of nonlinearity and dispersion of order ϵ for the initial data $u_0 = \beta \text{sech}^2 x$.

Introducing the slow time variable $\tau = t/\epsilon$, the fKdV case reduces to the standard fKdV equation

$$(47) \quad u_\tau + uu_x - D^\alpha u_x = 0,$$

which implies the dichotomy: either the solution is global or the blow-up time scales like the break-up time as $t \sim 1/\epsilon$. The numerical study here will be therefore performed only as a test of the numerical approach.

Alternatively, introducing the function $\tilde{u} = \epsilon u$, we get the equations

$$(48) \quad \tilde{u}_t + \tilde{u}\tilde{u}_x - \epsilon D^\alpha \tilde{u}_x = 0, \quad \tilde{u}_0 = \epsilon u_0$$

and

$$(49) \quad \tilde{u}_t + \tilde{u}_x + \tilde{u}\tilde{u}_x + \epsilon D^\alpha \tilde{u}_t = 0, \quad \tilde{u}_0 = \epsilon u_0.$$

Both (48) and (49) will be solved for the initial data $\tilde{u}_0 = \epsilon \beta \text{sech}^2 x$ for several values of ϵ . For $\epsilon = 0$, both equations reduce to the Burgers equation. For the initial data \tilde{u}_0 , the solutions to the Burgers equation have a point of gradient catastrophe, a hyperbolic blow-up, at the critical time

$$(50) \quad t_c = \frac{3^{3/2}}{4\beta\epsilon}.$$

Obviously the critical time t_c is of order $1/\epsilon$. We will now study for several ϵ for examples, for which we observed blow-up in the previous sections, how the time t^* scales with ϵ .

We first consider fKdV with $\alpha = 0.2$ for the initial data $\epsilon \text{sech}^2 x$ for the values $\epsilon = 0.01, 0.02, \dots, 0.1$. Since the blow-up is exponential, we just take the time for which the code stops converging as the blow-up time. This gives a very good approximation to t^* , and what is important since we are interested in the ϵ dependence, a consistent one for all ϵ . The computation is carried out with $N = 2^{16}$ Fourier modes for $x \in [-20\pi, 20\pi]$ and $N_t = 10^4$ time steps. Doing a linear regression analysis for $\log_{10} t^* \sim a \log_{10} \epsilon + b$, we find that the blow-up time t^* is as the time t_c (50) of order $1/\epsilon$. More precisely we get $a = -0.9998$, $b = 0.4845$ with standard deviation $\sigma_a = 2.1 * 10^{-4}$ and correlation coefficient $r = 9 * 10^{-8}$. Thus the expected dependence $t^* \propto 1/\epsilon$ is numerically well observed.

A corresponding analysis for fBBM is much more involved for two reasons: first the initial peak travels to the right before blowing up, the farther the smaller ϵ , whereas blow-up for fKdV happens close to the initial maximum. And secondly the blow-up is not as pronounced in fBBM as in fKdV for $\alpha < 0.5$. Thus it is less obvious to obtain an estimate for the blow-up time than for fKdV. The first problem is addressed as in (27) and (30) by using a frame commoving with the location of the maximum $x_m(t)$. Thus we solve

$$U_t - VU_y + (1 + \epsilon D^\alpha)^{-1}(U_y + UU_y) = 0,$$

where

$$V = \frac{(1 + \epsilon D^\alpha)^{-1}(U_y + UU_y)}{U_{yy}} \Big|_{y=0}.$$

To determine the blow-up time, we use the approach [48, 31] based on a fitting of the asymptotic behavior of the Fourier coefficients. We again use the initial data $U_0 = \epsilon \operatorname{sech}^2 x$ for the values $\epsilon = 0.01, 0.02, \dots, 0.1$. The computation is carried out with $N = 2^{15}$ Fourier modes for $x \in [-10\pi, 10\pi]$ and $N_t = 2 * 10^4$ time steps. Doing a linear regression as for fKdV, we find that the blow-up time t^* is again as the time t_c of order $1/\epsilon$. More precisely we get $a = -0.9677$, $b = 0.5521$ with standard deviation $\sigma_a = 0.005$ and correlation coefficient $r = 0.9999$. Thus we find again that the blow-up time t^* is proportional to $1/\epsilon$ as the break-up time t_c for the corresponding Burgers solution. Note that we always have $t^* > t_c$.

The above results therefore illustrates the fact that the life span of solutions of the Burgers equation

$$(51) \quad u_t + \epsilon u u_x = 0$$

is not enhanced by a weak dispersive perturbation having the same small coefficient ϵ . On the other hand, as we have seen in the previous subsection the blow-up is of a different nature than the shock type one of the Burgers equation.

When the small parameter ϵ affects only the quadratic term in (47), we have already noticed that the resulting equation reduces to the standard fKdV equation with initial data of order ϵ and our simulations suggest that for any $0 < \alpha < 1$ the solution is global for ϵ small enough.

4. OUTLOOK

The numerical results in this paper suggest that blow-up in solutions to fKdV equations when $1/3 < \alpha \leq 1/2$ is similar to blow-up in solutions to gKdV equations. In the L^2 critical case ($\alpha = 1/2$), the blow-up profile appears to be given by a rescaled soliton. In the L^2 supercritical case $1/3 < \alpha < 1/2$, the blow-up profile should be given by an asymptotically decreasing solution to the fractionary equation (32). To obtain further insight into this case, the asymptotics of solutions to this equation have to be worked out. It has to be shown whether there is a unique solution which is asymptotically decreasing. Then a numerical scheme has to be developed to compare the blow-up in fKdV solutions to a rescaled form of this particular solution to (32). This will be subject of further work.

Though the blow-up in the energy supercritical case $0 < \alpha < 1/3$ appears to be given by the same asymptotic profile, it is of a different nature due to the absence of solitary waves.

Another important question is related to the long-time behavior of solutions to fBBM equations for small nonlinearity as studied in the previous subsection. It would be worthwhile to investigate whether or not the found results persist in a more general context of dispersive perturbations of quasi-linear hyperbolic systems and of course for relevant water waves models such as the Boussinesq systems. In the latter case things might be more subtle

since the presence of a “BBM” term in the system weakens the nonlinearity in the corresponding equation.

Acknowledgements. *CK thanks for financial support by the ANR via the program ANR-09-BLAN-0117-01, JCS acknowledges partial support from the ANR project GEODISP.*

REFERENCES

1. J. ALBERT, J.L. BONA AND J.-C. SAUT, *Model equations for waves in stratified fluids*, Proc. Royal Soc. London A, **453**, (1997), 1233–1260.
2. C.J. AMICK, *Regularity and uniqueness of solutions of the Boussinesq system of equations*, J. Diff. Eq., **54** (1984), 231–247.
3. J. ANGULO, C. BANQUET AND M. SCIALOM, *The regularized Benjamin-Ono and BBM equation: well-posedness and nonlinear stability*, J. Diff. Eq. **250** (2011), 4011–4036.
4. J. L. BONA, T. COLIN AND D. LANNES, *Long-wave approximation for water waves*, Arch. Ration. Mech. Anal., **178** (2005), 373–410.
5. J. L. BONA, M. CHEN AND J.-C. SAUT, *Boussinesq equations and other systems for small-amplitude long waves in nonlinear dispersive media I : Derivation and the linear theory*, J. Nonlinear Sci., **12** (2002), 283–318.
6. J.L. BONA, V.A. DOUGALIS, O.A. KARAKASHIAN AND W.R. MCKINNEY, *Conservative, high-order numerical schemes for the generalized Korteweg-de Vries equation*, Philos. Trans. Roy. Soc. London Ser. A **351**, 1695 (1995), 107–164.
7. J.L. BONA AND J.-C.SAUT, *Dispersive blow-up of solutions of generalized Korteweg-de Vries equations*, J. Diff. Eqs., **103** (1993), 3–57.
8. J.L. BONA AND J.-C.SAUT, *Dispersive Blow-Up II : Schrödinger type equations*, Optical and Oceanic Rogue Waves, Chinese Annals of Math. Series B, **31**, (6), (2010), 793–810.
9. A. CASTRO, D. CÓRDOBA AND F. GANCEDO, *Singularity formation in a surface wave model*, Nonlinearity, **23** (2010), 2835–2847.
10. A. CONSTANTIN AND J. ESCHER, *Wave breaking for nonlinear nonlocal shallow water equations*, Acta Math., **181** (1998), 229–243.
11. M. EHRLSTRÖM, M.D. GROVES AND E. WAHLÉN, *On the existence and stability of solitary-wave solutions to a class of evolution equations of Whitham type*, Nonlinearity **25** (2012), 2903–2936.
12. M. EHRLSTRÖM AND H. KALISH, *Traveling waves for the Whitham equation*, Diff. Int. Equations **22** (11-12) (2009), 1193–1210.
13. P. FELMER, A. QUAAS AND J. TAN, *Positive solutions of the nonlinear Schrödinger equation with the fractional Laplacian*, Proc. Roy. Soc. Edinburgh, **142 A**, (2012), 1237–1262.
14. R.L. FRANK, *On the uniqueness of ground states of non-local equations*, arXiv:1109.4049v1, 19 Sep 2011.
15. R.L. FRANK AND E. LENZMANN, *On the uniqueness and nondegeneracy of ground states of $(-\Delta)^s Q + Q - Q^{\alpha+1} = 0$ in \mathbb{R}* , arXiv: 1009.4042 (2010)
16. J. GINIBRE AND G. VELO, *Commutator expansions and smoothing properties of generalized Benjamin-Ono equations*, Ann. Inst. Henri Poincaré, Phys. Théorique, **51** (1989), 221–229.
17. J. GINIBRE AND G. VELO, *Smoothing Properties and Existence of Solutions for the Generalized Benjamin-Ono Equations*, J. Diff. Eq. **93** (1991), 150–212.
18. S. HERR, A.D. IONESCU, C.E. KENIG AND H. KOCH, *A para-differential renormalization technique for nonlinear dispersive equations*, Comm. P.D.E. **35** (10) (2010), 1827–1875.
19. M. HOCHBRUCK, A. OSTERMANN, *Exponential integrators*, Acta Numerica **19** (2010) 209–286.
20. J.K. HUNTER AND M. IFRIM, *Enhanced lifespan of smooth solutions of a Burgers-Hilbert equation*, SIAM J. Math. Anal. **44** (3) (2012), 2039–2052.
21. J.K. HUNTER, M. IFRIM, D. TATARU AND T.K. WONG, *Long time solutions for a Burgers-Hilbert equation via a modified energy method*, arXiv: 1301.1947v1 9 Jan 2013.
22. V. M. HUR, *On the formation of singularities for surface water waves*, Comm. Pure Appl. Math. **11** (2012), 1465–1474.
23. M.A. JOHNSON, *Stability of small periodic waves in fractional KdV type equations*, arXiv: 1210.2326v1, 8 Oct 2012.

24. T. KAPITULA AND A. STEFANOV, *A Hamiltonian-Krein (instability) index theory for KdV-like eigenvalue problems*, preprint 2013.
25. A.-K. KASSAM, L.N. TREFETHEN, *Fourth order time-stepping for stiff PDEs*, SIAM J. Sci. Comput. **26** (4) (2005) 1214-1233.
26. T. KATO, *The Cauchy problem for quasi-linear symmetric hyperbolic systems*, Arch. Rat. Mech. Anal. **58**, (1975), 181–205.
27. A. KISELEV, F. NAZAROV AND R. SHTERENBERG, *Blow Up and Regularity for Fractal Burgers Equation*, Dynamics of PDE, **5** (3) (2008), 211–240.
28. C. KLEIN, *Fourth order time-stepping for low dispersion Korteweg-de Vries and nonlinear Schrödinger equations*, ETNA **29** (2008) 116-135.
29. C. KLEIN AND R. PETER, *Numerical study of blow-up in solutions to generalized Korteweg-de Vries equations*,
30. C. KLEIN, K. ROIDOT, *Fourth order time-stepping for Kadomtsev-Petviashvili and Davey-Stewartson equations*, SIAM J. Sci. Comput. **33** (6) (2011) 3333-3356. preprint (2013).
31. C. KLEIN, K. ROIDOT, *Numerical study of shock formation in the dispersionless Kadomtsev-Petviashvili equation and dispersive regularizations*, Physica D, 10.1016/j.physd.2013.09.005 (2013).
32. E.A. KUZNETSOV AND V.E. ZAKHAROV, *Nonlinear coherent phenomena in continuous media*, in *Nonlinear Science at the Dawn of the 21st Century*, P.L. Christiansen, M.P. Sorensen and A.C. Scott (Eds), Springer Notes in Physics, Springer-Verlag, (2000), 3–45.
33. J. C. LAGARIAS, J. A. REEDS, M. H. WRIGHT, P. E. WRIGHT, *Convergence properties of the Nelder-Mead simplex method in low dimensions*, SIAM Journal of Optimization **9** (1998) 112-147.
34. D. LANNES, *Water waves: mathematical theory and asymptotics*, *Mathematical Surveys and Monographs*, vol 188 (2013), AMS, Providence.
35. D.LANNES AND J.-C. SAUT, *Remarks on the full dispersion Kadomtsev-Petviashvili equation*, Kinetic and Related Models. AIMS, **9**, (4) (2013), 989-1009.
36. F. LINARES, D. PILOD AND J.-C. SAUT, *Well-posedness of strongly dispersive two-dimensional surface waves Boussinesq systems*, SIAM J. Math. Anal. **44** (6), (2012), 4165–4194.
37. F. LINARES, D. PILOD AND J.-C. SAUT, *Dispersive perturbations of Burgers and hyperbolic equations I : local theory*, arXiv:1302.7146v1 [math.AP] 28 Feb 2013, SIAMJ. Math.Anal., to appear.
38. Y. MAMMERI, *Long time bounds for the periodic Benjamin-Ono BBM equation*, Nonlin. Ana. TMA **71** (10) (2009), 5010–5021.
39. Y. MARTEL AND F. MERLE, *Blow up in finite time and dynamics of blow up solutions for the L^2 -critical generalized KdV equation*, J. Amer. Math. Soc. **15** (3) (2002), 617–664.
40. Y. MARTEL, F. MERLE, P. RAPHAËL, *Blow up for the critical gKdV equation I: Dynamics near the soliton*, Preprint available at: arXiv:1204.4625.
41. M.MING, J.-C.SAUT AND PING ZHANG, *Long time existence of solutions to Boussinesq systems*, SIAM J. Math. Analysis, **44** (6) (2012), 4078-4100.
42. P.I. NAUMKIN AND I.A. SHISHMAREV, *Nonlinear Nonlocal Equations in the Theory of Waves*, Translations of Mathematical Monographs, vol. 133, AMS Providence 1994.
43. Y. SAAD AND M. SCHULTZ, *GMRES: A generalized minimal residual algorithm for solving nonsymmetric linear systems*, SIAM J. Sci. Stat. Comput., **7** (3) (1986), 856-869.
44. J.-C. SAUT, *Sur quelques généralisations de l'équation de KdV I*, J. Math. Pures Appl., **58**, (1979), 21–61.
45. J.-C. SAUT AND LI XU, *The Cauchy problem on large time for surface waves Boussinesq systems*, J. Math.Pures Appl. **97** (2012), 635–662.
46. J.-C. SAUT AND LI XU, *Well-posedness on large time for a modified full dispersion system of surface waves*, J. Math. Phys. **53**, 115606 (2012).
47. M.E. SCHONBEK, *Existence of solutions for the Boussinesq system of equations*, J. Diff. Eq., **42** (1981), 325–352.
48. C. SULEM, P. SULEM, AND H. FRISCH, *Tracing complex singularities with spectral methods*, J. Comp. Phys., **50** (1983), pp. 138-161.
49. C. SULEM, P.-L. SULEM, *The nonlinear Schrödinger equation. Self-focusing and wave collapse*, vol. 139 of Applied Mathematical Sciences, 1st ed., Springer, 1999.
50. G.B. WHITHAM, *Linear and nonlinear waves*, Wiley, New York 1974.
51. LI XU, *Intermediate long waves systems for internal waves*, Nonlinearity **25** (2012), 597–640.

52. A. A. ZAITSEV, *Stationary Whitham waves and their dispersion relation*, Sov.Phys. Doklady **31** (1986), 118–120.

INSTITUT DE MATHÉMATIQUES DE BOURGOGNE, UNIVERSITÉ DE BOURGOGNE, 9 AVENUE ALAIN SAVARY, 21078 DIJON CEDEX, FRANCE, E-MAIL CHRISTIAN.KLEIN@U-BOURGOGNE.FR

LABORATOIRE DE MATHÉMATIQUES, UMR 8628, UNIVERSITÉ PARIS-SUD ET CNRS, 91405 ORSAY, FRANCE, E-MAIL JEAN-CLAUDE.SAUT@MATH.U-PSUD.FR